Review

Not peer-reviewed version

Mathematical Morphology-Based Fault Diagnosis to Rotating Machinery: A Review

Tingkai Gong , Xiaohui Yuan * , Bing Ji , Zhinong Li

Posted Date: 11 December 2025

doi: 10.20944/preprints202512.0987.v1

Keywords: mathematical morphology; morphology pattern spectrum; morphological wavelet; fault diagnosis; rotating machine; vibration signal

 doi:10.20944/preprints202512.0987.v1

Review

Mathematical Morphology-Based Fault Diagnosis to Rotating Machinery: A Review

Tingkai Gong [1], Xiaohui Yuan [2,*], Bing Ji [3] and Zhinong Li [4]

[1] School of Civil Aviation, Nanchang Hangkong University, NanChang, 330063, China
[2] School of Hydropower and Information Engineering, Huazhong University of Science and Technology, Wuhan, 430074, China
[3] School of Traffic and Transportation Engineering, Central South University, ShaChang, 410075, China
[4] School of Instrument Science and Optoelectronic Engineering, Nanchang Hangkong University, NanChang, 330063, China
* Correspondence: yxh71@hust.edu.cn

Abstract

Rotating machinery is crucial element in mechanical equipment, and during serving cycle their failure is inevitable because of artificial and non-artificial reasons. Signal processing techniques are available to diagnose the failure. Due to the nonlinearity and simplicity in computation rules and the richness in theoretical system, mathematical morphology (MM) has received significant research attention in this area, and numerous papers had been published in academic journals, conference proceedings, etc. The review paper attempts to overview the morphological framework and to summarize these applications grouped as rolling element bearing and gear. Finally, the relevant discussions on MM are analyzed, and several potential prospects are suggested.

Keywords: mathematical morphology; morphology pattern spectrum; morphological wavelet; fault diagnosis; rotating machine; vibration signal

1. Introduction

Rotating machinery is a significant component of modern industrial system, and plays important role in industrial applications. As a complex system, it is composed of various rotating parts to different aims, for example bearings are to support axis and/or radius loads, while gears are generally to change input speed or motion direction, etc. In most cases, their working conditions are quite harsh, such as high temperature and pressure, and time-varying in load and/or speed. Hence, the failure of rotating components is unavoidable, impairing the reliability and applicability of the mechanical equipment. Condition monitoring to the mechanical systems, especially the key rotating parts, has become an efficient and available solution scheme in theoretical studies and engineering applications [1,2].

The vibration measurement is most sensitive to the mechanical component faults, directly showing the information associated with abnormal conditions. However, the collected vibration signals are quite often nonstationary and nonlinear due to signal amplitude or/and frequency demodulation induced by time-varying effect. Meanwhile, additive-noise disturbance from background environment is embedded into such signals, increasing the difficult to detect these faults. Targeted this problem, different signal processing methods are considered, such as short time Fourier transform (STFT) [3–7] wavelet analysis [8–12], empirical mode decomposition (EMD)-based method [13–17] and variational mode decomposition (VMD) [18–23], etc. As we know, these methods have individual merits and demerits, for instance STFT can locate the change of interested signal components simultaneously in time and frequency but cannot obtain the optimal resolution because of Heisenberg uncertainty principle; the EMD-based method is a special model without basis function

 doi:10.20944/preprints202512.0987.v1

definition and suitable to process non-stationary signal but has mode mixing, end effect and the sensitivity to noise; VMD amends EMD but depends on the mode number and penalty coefficient highly.

It should be said that mathematical morphology is an interesting and robust theory. Firstly, it completes the successful crossing from image area to signal one. If saying that the crossing benefit only nonlinear filtering, the self-extension and the horizontal-extension (i.e., combining morphology with other theories) show the robustness, because the former unify the qualitative analysis with quantitative analysis for a specified target like fault diagnosis, and the latter retain the individual merit between two theories, such as morphological wavelet that has not only the nonlinearity of morphology, but also the multiresolution of wavelet. The theory framework is showed in figure 1. The merit melting maybe gives better explaining to a specified problem. As a result, morphology model provide a multi-view to rotating machine fault diagnosis.

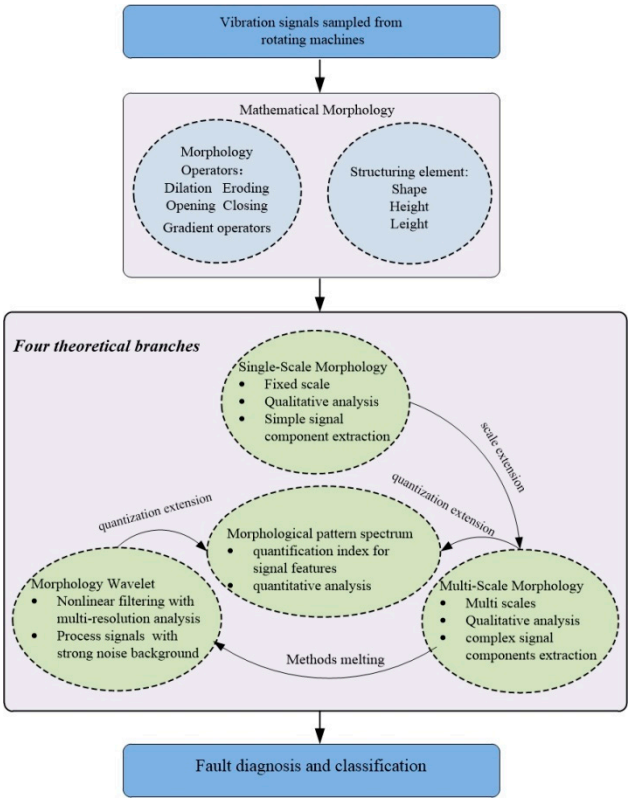

Figure 1. The framework to mathematical morphology.

Like most signal processing methods, mathematical morphology has its own working mechanisms. Firstly, it just involves simple computation rules, such as addition, subtraction and extrema solving, which are totally different to inner-product operation in Fourier transform (FT) and wavelet transform, allowing the change of the local details of signal to be observed visually. This brings more controllability in actual applications and is easily performed on hardware platform with lower computation cost. Besides, as a referred object or an information carrier, structuring element (SE) in morphology is more or less identical to the basic functions in Fourier and wavelet transform or window functions in STFT, and is designed by sampling point stacking as a specified shape. Obviously, the stacking definition to SE is completely different to the mathematical formula definition in conventional signal processing area. To a signal shape that is explicit to us, the stacking pattern, relatively speaking, can well describe both the integrity and the local variation of a signal, while the formulation one emphasizes the commonality for the shape. Therefore, the processing mechanisms maybe offers a more flexible solving scheme to improve fault diagnosis effect.

 doi:10.20944/preprints202512.0987.v1

For these reasons, enormous publications on mathematical morphology applied in rotating machine fault detection area occur in academic journals, conference proceedings and technical reports, etc. This paper makes an attempt to summarize and retrospect the current studies, allowing interested researchers to acquire relatively apparent level on mathematical morphology. The remaining part of the paper is structured as follows. Section 2 presents morphological foundation about morphological operators, structuring element and four morphology-based methods. Section 3 introduces the reference review on morphological applications in rotating machinery fault diagnosis, followed by a brief discussion and potential prospects in Section 4. Section 5 describes some concluded remarks.

2. Mathematical Morphology

Morphological theory is developed based on set theory, topology, stochastic geometry, lattice theory, and nonlinear partial differential equations, etc. [24–26]. In image processing field it can complete image segmentation [27–31], image feature extraction [32–37], edge detection [38–41] and image enhancement [42–45]. Due to the nonlinear filtering and strong signal demodulation behavior, it is gradually extended into 1D signal processing [46–48].

Mathematical morphology is an interactive behavior between structuring element and a signal as certain computation rules, with a goal that is to remove irrelevant contents and retain pivotal detail. It involves two important factors: morphology operator and structure element. The former defines the mathematical computation rules, while the latter is a reference object or an information carrier that is expected to be extracted from a processed signal or image.

2.1. Morphological Operator

Morphology theory includes four basic operators, i.e., dilation, erosion, opening and closing. Let f(n) be one-dimensional signal with a domain at F = (0, 1, 2, …, N-1), and s(n) be a structuring element with at a domain at S= (0, 1, 2, …, M-1) (M << N). Then dilation and erosion are formulated as:

$$(\mathrm{f} \oplus \mathrm{s})(\mathrm{n}) = \max\{\mathrm{f}(\mathrm{n}-\mathrm{m}) + \mathrm{s}(\mathrm{n})\} \quad \mathrm{m} \in 0,1,2 \cdots \mathrm{M}-1 \tag{1}$$

$$(f \ominus s)(n) = \min\{f(n+m) - s(n)\} \quad m \in 0,1,2 \cdots M-1 \tag{2}$$

where $\oplus$ and $\ominus$ represent dilating and eroding, respectively. Because dilation and erosion are similar to addition and subtraction in arithmetic, they can extent or shrink the morphological shapes of image. It is noteworthy that the two operators in practical applications cannot restore original image, thus closing and opening are defined as:

$$(f \cdot s)(n) = (f \oplus \mathrm{s} \ominus \mathrm{s})(\mathrm{n}) \tag{3}$$

$$(f \circ \mathrm{s})(n) = (f \ominus s \oplus s)(n) \tag{4}$$

where $\circ$ and $\bullet$ stand for opening operation and closing operation, respectively. Toward a one-dimensional signal, morphological operations have specified computation rules, for instance, dilation and erosion separately solve local max and minimum values. Based on Eqs.(3) and (4), closing detects local max then minimum and opening is inverse performance.

On the other hand, the dynamic feature of signal is complex during sampling time, but basic operators have single performance to identify such features (the reason will be explained subsequently). In order to improve the situation, except for the four basic operators, morphological gradient operators are constructed as a combination between them. For example, the difference between closing and opening (DCO) and the difference between dilation and erosion (DDE) are given as follows:

$$DCO(f) = (f \oplus s \ominus s)(n) - (f \ominus s \oplus s)(n) \tag{5}$$

 doi:10.20944/preprints202512.0987.v1

$$DDE(f) = (f \oplus s)(n) - (f \ominus s)(n) \tag{6}$$

In order to distinguish the difference in extracting signal feature for these operators, a simulation analysis is considered. Here, a linear flat SE with the length of 5-sampling-point is utilized to simplify the discussion.

Figure 2(a) is the result of dilation, showing that the signal peaks are smoothed and the valleys are extended upward, i.e., the signal waveform is almost shifted upward. In fact, the performance depends on three factors, the computation rule of dilation operator, the SE length and the location of the dilated point. For example, when a data point near a peak is dilated, because the peak is biggest in the local area that is controlled by the SE length (the relation between the length and the locality will be explained in Section 2.2), this point is thus replaced by the peak. Following the SE movement, others near the peak will be also replaced and the peak extension happens, i.e., the peak area is flatted. Conversely, when one point near a valley is dilated, it possibly is replaced by a local max. Furthermore, when the valley bottom is dilated, there must be a bigger point in this local area, thus it will be replaced with the bigger point, that is, the whole valley area is shifted upward. If there are not local maxima around the currently dilated point, it keeps original status, for example the previous sampling points in Figure 2(a). According to the analysis, the dilation behavior to a signal is summarized as smoothing the signal peaks, retaining signal valleys, and making the signal waveform moved upwards. Differently, Erosion is to detect local minimum, resulting in a reverse performance as illustrated in Figure 2(b).

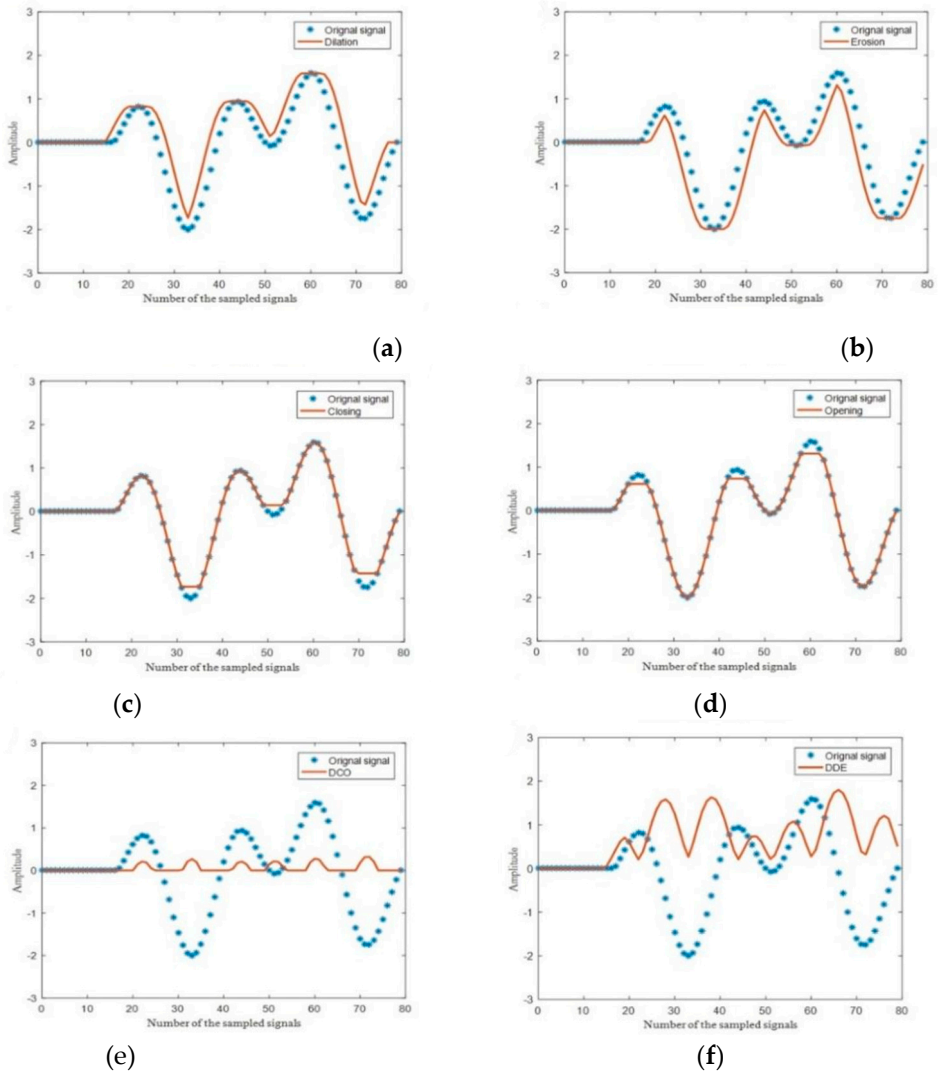

 doi:10.20944/preprints202512.0987.v1

Figure 2. Performance of morphological operators to a simulated signal. (a) Dilation, (b) Erosion, (c) Closing, (d) Opening, (e) DCO, (f) DDE.

Next, closing is analyzed. According to Eq.(3), it is a cascading model between dilation and erosion, thus the closing output in Figure 2(c) corresponds to eroding the waveform in Figure 2(a). And the date points at the special flatted and volley areas need be concerned, because normal points can be derived based on the performance of dilation and erosion to signal. For instance, when one point at the flatted peak is eroded, because there must be a minimum, it is replaced by the minimum. Following multi-erosion, the flatted peak area is gradually restored to original status. On the contrary, when a point near a valley is eroded, because the valley bottom is smallest in the local area, this point will be replaced by the valley bottom, that is, the valley region is smoothed during the eroding procedure. Consequently, closing operation to a signal can extract peaks and smooth valleys, and opening is the inverse performance displayed in Figure 2(d).

Among gradient operators, the operator DCO, relatively speaking, is analyzed easily. According to Eq.(5), the signal waveform in Figure 2(e) can be regarded as the difference computation between Figure 2(c) and Figure 2(d). Because the two figures are almost similar each other, only smaller peaks are obtained in Figure 2(e), where the flatted regions in Figure 2(c) are preserved, and the negative flatted regions Figure 2(d) are converted into the positive ones due to the difference computation. It indicates that the DCO operator can keep oscillation tendency in the signal. In comparison with DCO, DDE has more complex behavior presented in Figure 2(f), where the waveform oscillations quite often happen. This is mainly because the extrema in the signal are strongly random, meanwhile solving extrema through dilation and erosion is controlled by the SE length, thereby leading to the strong random oscillation.

According to the analysis above, it should be said that the morphological operation provide a microcosmic and intuitive view to observe or process a signal. As a result, it brings more controllability in theoretical study and actual applications.

2.2. Structuring Element

Structuring element acts as a moving window with specified shape to probe interested component in signal or image. It is designed as a matrix containing 1′ component and 0′ component. Thereinto, the former called neighborhood is located at some positions in the matrix to shape a specified figure with the assistance of the latter. In fact, structuring element itself is a given information carrier, then these morphological features in an object that are identical to the SE will be identified by the morphology processing.

Theoretically, SE is simpler in shape and smaller in size than those of the analyzed object, and comprises three physical properties, shape, length and height. The shape represents what geometric outline is concerned to us, and can be triangle, circle, disk, and rectangle, etc. If required, irregular shapes also can be defined. Moreover, the shape should contain detailed quantification in time scale and space scale, i.e., length and height. The former shows the shape in the time duration, and the latter indicates space extension. In general, the length is an integer number, and height is a real one. To practical applications, structuring element will be determined by the three parameters, but it does not mean that they all must be defined. In most cases, the first two properties need be considered, but the height can be neglected (i.e., setting as 0) because it can simplify morphological calculation. For this reason, it is grouped into two types, flat structuring element and non-flat structuring element. When flat SE is used, morphological operation just involves local extrema searching, while non-flat one is employed, the height values is introduced into morphological calculation by subtraction or addition, and then the obtained result performs extrema searching.

In order to show the difference when SE of different type is utilized, two examples are presented here. Assume that operator is dilation, and a flat SE is set as {1 $\underline{1}$ 1}, where the underlined element is an original point, which will be matched with data points from the first point to last one in a signal, i.e., the whole morphological operation is conducted when it is matched with the last. For example,

 doi:10.20944/preprints202512.0987.v1

when the origin is matching with the point x_i of the signal X in Figure 3, it means that x_i is dilating, and the current dilation is the max among three points (i.e., x_{i-1}, x_i, x_{i+1}) because the SE length is three-sampling-point. Until such matching happens at the last point, the eventual dilation result is obtained. On the other hand, if SE is {1 1 0}, the output of dilating x_i is the max between the two points x_{i-1} and x_i, rather than the three points. Because the point x_{i+1} corresponds to the 0′ component in the SE, it cannot be involved into the current dilation. As a result, 1′s component in structure element depends on how many data point will be introduced in a morphological calculation, while 0′s component assists 1′s component to construct a specified shape.

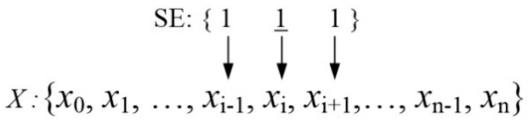

Figure 3. Morphology dilation.

When a non-flat SE is defined as [{1, 1, 1}, {h_0, h_1, h_2}], where h_i is the corresponding height. In the same way, when the point x_i is dilated, firstly x_i adding h_i is performed, i.e., the new three points $x_{i-1}+h_0$, x_i+h_1, $x_{i+1}+h_2$ are obtained, and the current dilation output is the max among them. It indicates that when a non-flat SE is used, the morphology operation is firstly addition/subtraction (when using erosion) between data points and the SE heights and then solves extrema.

It is clear that SE determines the computation range in a morphological processing, and highly dominates the result when compared with morphological operators. As stated in Introduction, a merit of morphology is nonlinear filtering performance. Based on the viewpoint, it should be known that a small SE is beneficial to preserve morphological features but unbeneficial to remove noise, and vice versa.

2.3. Introduction to Morphology-Based Methods

Mathematical morphology is a broad systemic framework, following the development, four methods based on the morphology are introduced, i.e., single-scale morphology (SSM), multi-scale morphology (MSM), morphological pattern spectrum (MPS) and morphology wavelet (MW).

2.3.1. Single-Scale Morphology

SSM means that just one structuring element is utilized. As we know, the SE definition is very flexible. To obtain better processing, sometimes different SEs will be used, but the optimal one is eventually considered by certain selection criterion. In this case, it still belongs to the SSM analysis.

Relatively speaking, the single-scale analysis is simpler in applications, for instance when flat SE is considered, the length is only defined and its reasonability is certainly quite crucial. Otherwise, the analysis easily suffers from under- or over-processing. In general, SSM is suitable to process the signal that does not contain multiple signal components, because it is hard to well match the morphology features between single SE and a complex signal. As a result, how to construct proper SE in SSM is most important to the expected processing result.

2.3.2. Multi-Scale Morphology

In a real environment, the measured signal is complicated, possibly containing different signal components. Based on the morphological features matching, it is expected that using different scales allows each signal component to be isolated into individual corresponding scale. Accordingly, the multi-scale technique has comprehensive analysis ability and is suited to deal with such complex signal.

 doi:10.20944/preprints202512.0987.v1

In the Multi-scale model, varying scales are achieved by self-dilation of unit scale. In this situation, it produces two advantages, enhancing computation efficiency and simplifying morphology calculation.

Let γ (γ=1,2,3…γ_{max}) be the scale parameter, and s be unit SE. The SE at scale γ can be given as

$$\gamma s = \underbrace{s \oplus s \oplus \cdots s \oplus s}_{\gamma-1\ times} \tag{7}$$

According to the definition above, the dilation and erosion operators of signal $f(x)$ at scale γ are written as

$$f \oplus \gamma s = \underbrace{f \oplus s \oplus \cdots s \oplus s(n)}_{\gamma-1\ times} \tag{8}$$

$$f \ominus \gamma s = \underbrace{f \ominus s \ominus \cdots s \ominus s(n)}_{\gamma-1\ times} \tag{9}$$

And the closing and opening operators of signal $f(x)$ at scale γ can be separately formulated as:

$$f \cdot \gamma s = \mathrm{f} \oplus \gamma s \ominus \gamma s(\mathrm{n}) \tag{10}$$

$$f \circ \gamma s = f \ominus \gamma s \oplus \gamma s(n) \tag{11}$$

Similarly, morphological gradient operators DCO and DDE at scale γ are represented as

$$DCO(f)_{\gamma} = (f \cdot \gamma s)(n) - (f \circ \gamma s)(n) \tag{12}$$

$$DDE(f)_{\gamma} = (f \oplus \gamma s)(n) - (f \ominus \gamma s)(n) \tag{13}$$

Toward the multi-scale analysis, two problems need to be noticed. Firstly, the used scales are generally continuous, and according to the effect of the SE scale to morphology result (i.e., small scale is beneficial to retain the morphological features of signal but unbeneficial to clear noise), the scales also require proper definition, otherwise an over- or under- analysis will happen. On the other aspect, the core to MSM is the diversity among all scales used, each signal component in a signal has stronger correlation with corresponding scale, and the final signal is reconstructed by the results of the whole or part of the used scales.

2.3.3. Morphological Pattern Spectrum

In image processing field, the shape representation and the shape-size description are key tasks, because the former shows qualitatively that an image contains what important information, and the latter replies quantitatively that how many such one is covered in the image. However, SSM and MSM work through structuring element moving inside an object, just answering that the SE is contained or not in the object, thus essentially they are qualitative analysis. As mentioned above, the quantitation of specific information facilitates more accuracy estimation and understanding to image, thereby Maragos presented morphological pattern spectrum [49,50], which is also called granulometric analysis in image processing area by a sieving procedure to extract size distributions [51–54].

Morphology pattern spectrum is composed of two terms, morphology pattern and spectrum. Morphology pattern represents a particular prototype shape that is maybe contained in one object, and spectrum is a quantized evaluation to the shape pattern. Obviously, when the “spectrum” is discussed, it allows us to associate with the idea spectrum in Fourier transform. In fact, there exists certain similarity between them. In order to understand MPS well, the Fourier transform (FT) is described here.

As we know, the FT of a signal f(t) is defined as $F(\omega) = \int_{-\infty}^{\infty} f(t)e^{-i\omega t}dt$, noticing that the signal spectral component is calculated through a modulation $f(t)e^{-i\omega t}$ between f(t) and complex sinusoid $e^{-i\omega t}$. For instance, when a frequency ω is defined, the spectral component is obtained by measuring the

 doi:10.20944/preprints202512.0987.v1

area of the modulation. Following ω varying over a certain interval, the whole spectral will be produced. It is clear that the complex signal $e^{-i\omega t}$ works as a probing pattern with a series of spectrum component ω, and they can be extracted by the interactions between the complex signal and a processed signal. According to the transform, it can tell us that ω exists or not in the signal, but the details like shape and shape-size of $e^{-i\omega t}$ is missed.

In order to construct MPS by FT, corresponding concepts should be modified. for example, one-dimension signal $s(t)$ is transformed into two-dimension image X, the complex signal $e^{-i\omega t}$ corresponds to structuring element S_n, where subscript n defines S as a specified shape with certain size, and converting the signal modulation as the shape-size transformation of X. Then the area of a transformed image is calculated to obtain MPS of X by measuring the size distribution for X relative to S_n. For example, the area measuring to X by opening is defined as a normalized version:

$$F(r) = A(X \circ rS)/A(X) \tag{14}$$

where notation $A(\bullet)$ means area solving, and numerator and denominator stand for the areas of opening and the original image X, respectively. As we know, the area of the image $A(X)$ is fixed, but the area $A(X \circ rS)$ varies following the change of r. Considering from probability theory, the function $F(r)$ represents the probabilistic measures of the size distribution relate to S of size r in image X. Besides, the probing pattern rS will translate in the image, thus such area solving shows cumulative distribution property.

Based on the area measurement above, MPS can be defined as differential size distribution:

$$MPS_X(r, S) = -dA(X \circ \mathrm{rS})/dr \quad r \geq 0 \tag{15}$$

It represents the union that contains all patterns of X that are relative to size r. Furthermore, varying S or r, it can obtain different information, for example, if S is shaped as various figures with a fixed r, MPS indicates that the image most resembles which one. If S is fixed but r changes, it means all size components in the image. Additionally, Convexity of S implies that MPS is nonnegative for all $r \in R$ due to $X \circ rS \supseteq X \circ lS$ if $r \leqslant l$, thus MPS is the non-negativity when increasing r.

On the other hand, probing pattern $e^{-i\omega t}$ in FT has a positive frequency component ω. In fact, the probing pattern also can be $e^{i\omega t}$, corresponding to negative frequency component $-\omega$. It is the same as MPS, that is, when negative scale $-r$ is used in closing, MPS is written as:

$$MPS_X(-\gamma, s) = dA(X \cdot rs)/dr \quad r > 0 \tag{16}$$

Viewing from image processing and set theory, the positive scale is to process the umbra of an image, whereas the negative scale is to process the complementary of the umbra of the image.

Due to the consecutiveness of r according to Eq.(16), it is hard to use an analytical way to compute MPS, thus the discrete-form MPS is given as:

$$MPS_f(+n, s) = A[f \circ ns - f \circ (n+1)s] \quad 0 \leq n \leq N \tag{17}$$

$$MPS_f(-n, s) = A[f \cdot ns - f \cdot (n-1)s] \quad 1 \leq n \leq K \tag{18}$$

where N is the max size n, and K is the minimum size n. In two equations, $A(f) = \sum_{(x,y)} f(x, y)$, and notation $(a - b)(x) = a(x) - b(x)$ refers to an algebraic difference between $a(x)$ and $b(x)$. $A(f)$ is calculated by the difference between closing or opening using two approaching scales.

As we know, MPS is a further development in mathematical morphology, whose basis is set theory. Based on this point, it can be considered as a mapping relationship between two compact sets, i.e., set $A = \{H_1, K_2, H_3, \cdots H_n\}$ and structuring elements set$\Theta = \{S_1, S_2, S_3 \cdots S_m\}$. Then, the area measuring by SE in set Θ constructs a mapping on set A that is defined as $P_\Theta(H_i) = \{X_{i1}, X_{i2}, X_{i3}, \cdots, X_{im}\}$, where morphological pattern spectrum X_{ij} for Hi in set A is produced by set Sj. It means that if and only if $P_\Theta(H_i) \neq P_\Theta(H_m)$ when i ≠m, P_Θ is an invertible mapping on set A, that is, the shapes in A is completely distinguished by the measurement.

 doi:10.20944/preprints202512.0987.v1

When a shape pattern is utilized, the probabilistic measures reflect its size distribution by area solving. It means that the defined pattern is qualitative information, and the measure represents quantitative descriptor. On the other hand, the pattern information of rotating parts with different faults is otherness, thus the pattern spectrum provides a new view as classification tool to rotating part faults.

2.3.4. Morphological Wavelet

In a real world, the features of signal are in general both scale- and resolution-varying and highly nonstationary in space. Researchers recognized that multiresolution signal decomposition is fairly significant to theoretical developments and practical applications, because it makes these features represented at different scales, with efficient and clear understanding to such signal and with high computational advantages.

As a classical multiresolution technique, traditional wavelet transforms (TWT), termed first-generation wavelet, is based on Fourier transform and z transform to design a filter bank with special properties that are homologous with the multiresolution, for example such applications in the signal and image processing applications [8–12]. It is known that TWT is linear processing method like signal scaling, but the linear model is may not be compatible with attributes of interest, for example blurring the edge information of signal or image. Hence, scholars made contribution to attempt a theoretical extension from linear to nonlinear for the multiresolution analysis, expecting that the results obtained by this analysis varied in non-intuitive manner.

The extension is nonlinearity and wavelet-type multiresolution. The former means using nonlinear operators, such as dilation and erosion in mathematical morphology. At the same time, the multiresolution analysis is multi-level decomposition, i.e. a signal is analyzed and understood within different signal spaces, and should be an inverse process. Viewing from these points, the extension concerns two aspects, non-redundant to signal decomposition and perfect reconstruction to signal reconstruction. To satisfy the requirements, it actually experiences many trials.

In 1991, Pei and Chen [55,56] firstly put forward non-redundant nonlinear sub-band decomposition by using morphological theory, but it cannot perform perfect signal reconstruction. For this reason, Egger and Li [57] developed an improved method by means of median-type operation. And a similar study is found in literature [58]. Subsequently, Queiroz et.al. [59] proposed a type of nonlinear wavelet decomposition for lowing image code complexity. In 1997, Cha and Luis [60] used morphological opening operator to construct a nonlinear wavelet transform having perfect signal reconstruction. During the exploration process, these studies provide significant reference for future development, but do not present a general framework in morphology area to such nonlinear development. Differently, the traditional wavelet is done well at the same period, i.e., lifting scheme termed second-generation wavelet [61–63]. In order to understand the morphological wavelet well, lifting scheme is simply discussed here.

The so-called lifting is further development to these existing wavelets, i.e., using a new tool to construct them for analyzing signals that are defined in arbitrary domains, without the assistance of Fourier and z transform. It is divided into three steps, split, predicting and update. Firstly, a signal A_0 is split into two subsets, A_1 and B_1, i.e., the former is even samples with high approximation to the original signal, and the latter is odd samples with less information. Theoretically, a signal has some correlation structures in its sampling domain, thus it is instinctive to utilize a specified way to replace B_1 with A_1, i.e., prediction $B_1 = P(A_1)$, where P is predicting operator. In practice, it is hard to exactly predict B_1 by means of A_1, then the difference between B_1 and its prediction $P(A_1)$ is considered as.

$$B_1' = B_1 - P(A_1) \tag{19}$$

After n steps are conducted repeatedly, the original signal A_0 can be replaced with a subset $\{A_n, B_n, B_{n-1},\ldots,B_1\}$. Noting that the analysis is down-sampling, the last step will obtain a random sample, possibly appearing aliasing. It means that the globe property of the signal can't be preserved, e.g., mean. In order to deal with the problem, an update operator is introduced:

 doi:10.20944/preprints202512.0987.v1

$$A_1' = A_1 - U(B_1) \tag{20}$$

where U is updating operator. The procedure is the lifting scheme, and interested readers can refer [64–71]. Lifting scheme provides a general systemic framework that constructs those exiting wavelets. What's more, it also provides alternative idea for the nonlinear extension.

Inspired by the lifting scheme, Goustias and Heijmans [72,73] proposed an axiomatic framework morphological wavelet, in which morphological pyramid based on complete lattice is constructed as a type of nonlinear model to satisfy the multiresolution decomposition. The model presents two wavelet-type decompositions, nonlinear scheme called coupled wavelet decomposition and linear one called uncoupled wavelet decomposition. In practice, the morphological wavelet can be regarded as a special case of lifting scheme, namely prediction and update utilize morphological operators.

1. Coupled wavelet decomposition

To nonlinear signal decomposition cases, coupled wavelet decomposition is conducted by three operators, covering two analytical operators (one for the approximation signal and one for the detail signal) to perform multiresolution analysis and one synthesis operator to reconstruct signal.

Assume that V_j and W_j are signal space and detail space at level j, respectively. Then the signal decomposition is performed by analytical operators as increased direction through mapping level j into j+1, i.e., the analysis operator $\psi_j^{\uparrow}: V_j \longrightarrow V_{j+1}$, and the detail operator $\omega_j^{\uparrow}: V_j \longrightarrow W_{j+1}$. The analysis operator can obtain approximation or simplification of signal with many signal properties, while the detailed operator obtain a refinement. Reversely, the signal synthesis can be conducted by synthesized operator as decreased direction $\Psi_j^{\downarrow}: V_{j+1} \times W_{j+1} \longrightarrow V_j$. The one-stage decomposition is depicted in Figure 4 (a).

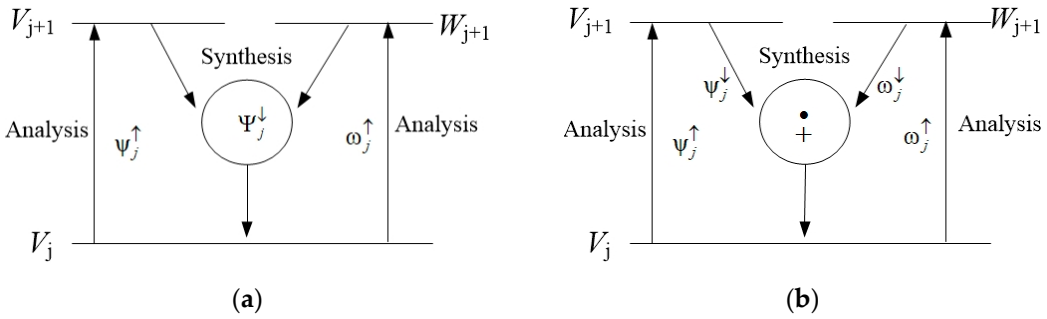

Figure 4. (a) Coupled-wavelet decomposition scheme. (b) Uncoupled-wavelet decomposition scheme.

On the other hand, a robust signal decomposition method requires certain constraint conditions to guarantee the non-redundancy in decomposition and the perfection in reconstruction. Therefore, when Eq.(21) and Eq.(22) are hold, the two requirements can be guaranteed. At the same time, the two conditions implicitly show that the mapping of operators is injective upward and surjective downward.

$$\Psi_j^{\downarrow}\left(\psi_j^{\uparrow}(x), \omega_j^{\uparrow}(x)\right) = x, if\ x \in V_j \tag{21}$$

$$\begin{cases} \psi_j^{\uparrow}\left(\Psi_j^{\downarrow}(x,y)\right) = x, if\ x \in V_{j+1}, y \in W_{j+1} \\ \omega_j^{\uparrow}\left(\Psi_j^{\downarrow}(x,y)\right) = y, if\ x \in V_{j+1}, y \in W_{j+1} \end{cases} \tag{22}$$

According to the decomposition scheme, a given signal $x_0 \in V_0$ can be decomposed in the recursive way as:

$$x_0 \to \{x_0, y_0\} \to \{x_1, y_1\} \to \{x_2, y_2, y_1\} \to \cdots \{x_k, y_k, y_{k-1}, \cdots y_1\} \to \cdots \tag{23}$$

On the other hand, the original signal can be completely rebuilt from these sub-signals x_k and y_1, y_2, $\cdots$ y_k by the synthesized scheme:

 doi:10.20944/preprints202512.0987.v1

$$x_j = \Psi_j^{\downarrow}(x_{j+1}, y_{j+1}), \qquad j = k-1, k-2, \cdots 0 \tag{24}$$

Hence, the signal decomposition scheme as Eqs. (20) - (23) is called the coupled wavelet decomposition scheme.

2. Uncoupled wavelet decomposition

In morphology wavelet, uncoupled wavelet scheme is linear decomposition as a special case of the nonlinear decomposition, and the decomposition procedure is the similar as that of nonlinear one, only the signal synthetization will use a binary addition operation $\dot{+}$ to make Eq. (25) hold when $\psi_j^{\downarrow}: V_{j+1} \longrightarrow V_j$ and $\omega_j^{\downarrow}: W_{j+1} \longrightarrow V_j$. The two operators $\psi_j^{\downarrow}$ and $\omega_j^{\downarrow}$ are taken to the signal synthesizing and the detail synthesizing, respectively.

$$\Psi_j^{\downarrow}(x, y) = \psi_j^{\downarrow}(x) \dot{+} \omega_j^{\downarrow}(x) \quad x \in V_{j+1}, y \in W_{j+1} \tag{25}$$

Meanwhile, in the linear case Eq. (26) is perfect reconstruction condition, and Eq. (27) and Eq. (28) represent non-redundant decomposition conditions.

$$\psi_j^{\downarrow}\psi_j^{\uparrow}(x) \dot{+} \omega_j^{\downarrow}\omega_j^{\uparrow}(x) = x, \quad if\ x \in V_j \tag{26}$$

$$\psi_j^{\uparrow}(\psi_j^{\downarrow}(x) \dot{+} \omega_j^{\downarrow}(x)) = x, \quad if\ x \in V_{j+1}, y \in W_{j+1} \tag{27}$$

$$\omega_j^{\uparrow}(\psi_j^{\downarrow}(x) \dot{+} \omega_j^{\downarrow}(x)) = y, \quad if\ x \in V_{j+1}, y \in W_{j+1} \tag{28}$$

For a signal $x_0 \in V_0$, the reconstruction in recursive synthesis scheme is:

$$x_j = \psi_j^{\downarrow}(x_{j+1}) \dot{+} \omega_j^{\downarrow}(y_{j+1}) \quad j = k-1, k-2, \cdots, 1, 0 \tag{29}$$

It means that the signal x_j at level j is reconstructed as mapping-down by the standard addition of an approximation signal and a detail signal at level j+1. As a result, the signal representation process represented as Eqs. (22) - (27) is the uncoupled wavelet decomposition scheme illustrated in Figure 4 (b).

Morphological wavelet completes the nonlinear extension of TWT by using mathematical morphology, keeping the multiresolution analysis and emphasizing shape and edge preservation. It affords a flexible and versatile analysis to signal.

3. Application of Mathematical Morphology to Rotating Machine

As stated in Introduction, rotary mechanical parts, such as bearing and gear, are crucial main components of rotating machinery, and their working statuses quite often work as key referenced indicators that can directly evaluate the mechanical equipment with or without faults. Hence, diagnosis and classification to part faults are always academic study topic.

Once a defect happens on these rotating components, the vibration response embodies impulsive feature, whose strength depends on the defect size, load, input speed and other objective factors. Moreover, it probably triggers the systemic resonance of mechanical equipment or rotating components, resulting in the energy increase around these system inherent frequencies. On the other hand, the vibrational signal shows two characteristics. One is the modulation in amplitude, frequency and phase, or the combination between them under complicated running conditions. The modulation carriers can be the shaft or cage rotational frequency in bearing, and the meshing frequency or inherent frequencies of rotating parts in gear. Another characteristic is noisy contamination to the vibration signal from signal collecting environment, especially when the occurred failure is incipient, and it affects the diagnosis performance of the used methods significantly.

Aiming at bearing and gear fault diagnosis, the morphology-based approaches have conducted many theory explorations and achieve successful investigations. This section will present a synthetical summary on rotating machinery fault diagnosis, with a classification as single-scale morphology, multi-scale morphology, morphological pattern spectrum and morphological wavelet.

 doi:10.20944/preprints202512.0987.v1

Besides, a sub-classification in each method is given according to fault objects like bearing, gear and other mechanical fault detection.

3.1. Single-Scale Morphology-Based Rotating Parts Fault Diagnosis

SSM just uses an operator and a fixed SE to complete a morphological operation and is relatively simple in practical applications. Under the condition, the morphology filtering behavior highly relies on the physical properties of structuring element.

3.1.1. SSM to Detect Bearing Defect

Nikolaou and Antoniadis [74] firstly employed SSM to extract the impulsive signals from defective bearings. They analyzed the different properties of morphology operators to impulsive signals and experimentally defined a flat structure element length. Dong et al. [75] defined four fixed SE length and just used one of them for different bearing defects. The similar method that selects the length of flat SE is founded in Ref [76–79] when diagnosing bearing failure. In these studies, structuring elements are all defined by prior knowledge. In this case, the sampling frequency of raw signals and the noisy interference intensity all affected on morphological results, easily resulting in over- or under- filtering phenomena.

In order to deal with the problem, many scholars attempt to utilize some adaptive methods to construct SE. For instance, Yu et al. [80] defined the optimal length, when the amplitude of the first five feature frequencies of bearings is largest. Hu et al. [81] presented SE construction method according to the relationship between the bearing fault impulse and a harmonic function with the resonant frequency, harmonic waveform in a period. Differently, Hu et al [82] defined the SE length by the relationship between the vibration sampling rate and the frequency response. Wang et al. [83] believed that the impulses of defective bearing have attenuated attribute, and SE is thus modelled as an impulse attenuation function formulated by the max amplitude, natural frequency and decay rate of the structure element. Yan and Jia [84] presented morphological slice bispectrum fused with cuckoo searching for diagnosing bearing failure. Van et al. [85] used particle swarm optimization algorithm to obtain the SE length.

On the other hand, when the different lengths of SE are used in real applications, the filtered signals have different statistical properties in time- or frequency- or time-frequency domain, thus some evaluated indexes are introduced to determinate the optimal one of the SE lengths. For example, Dong et al. [86] and Raj et al. [87] presented the optimized algorithms separately based on signal to noise and kurtosis to obtain the optimal length of flat SE. Zhang et al. [88] calculated alpha stable distribution to optimize the flat SE length and demonstrated the optimization superiority in capturing bearing outer and inner fault characteristic frequencies when compared with the optimization based on kurtosis. Noting that the aforementioned studies only employed one indictor to define the structuring element length, sometimes considering the higher reliability, some researchers tend to use a combination way between multiple indicators to achieve the task. For instance, Osman et al. [89] and Lv et al. [90] designed a fusion indicator separately based on kurtosis and Renyi entropy, and kurtosis and Teager energy operator to select the optimal SE length, and the results demonstrated that it is effective and robust to incipient bearing fault detection. Li et al. [91,92] considered characteristic frequency intensity coefficient working with third-order cumulant slice spectrum and diagonal slice spectrum for defining the SE length in bearing fault feature extraction.

3.1.2. SSM to Detect Gear Defect

Feng et al. [93] applied four sampling points as the SE length in SSM to filter background noise from raw signals and calculated multi-fractal entropy to classify gear working statuses. Chen et al. [94] empirically defined the linear SE length to demodulate the gear fault features. Gryllias et al. [95] proposed SSM to perform gearing fault detection, in which SE is constructed a linear shape with the length of 0.6 times impulse cycle period.

 doi:10.20944/preprints202512.0987.v1

Lin et al. [96] developed a hybrid approach based on morphological filtering, wavelet theory and empirical mode decomposition to detect the incipient gear fault. Guo et al. [97] presented a combined scheme based on single scale morphology, where the optimal SE length is adaptively determined according to kurtosis and modulation signal bispectrum.

3.2. Multi-Scale Morphology-Based Rotating Parts Fault Diagnosis

MSM acts as an extension to SSM, thus it is more suitable to handle complex real signal. Essentially speaking, the multiscale analysis still considers establishing the corresponding relationship between the SE scales and the morphological feature of signal components. Based on the morphology filtering peculiarity (small scales are conducive to retaining useful information but non-conducive to suppressing noise, and vice versa), the effectiveness of MSM also depends on the reasonability to the used scales.

3.2.1. MSM to Detect Bearing defect

Li et al. [98] employed multiscale morphology with gradient operator and experimentally determined the length scales of flat SEs. Feng et al. [99] considered a hybrid scheme based on MSM and manifold learning to classify bearing flaws. Gong et al. [100] proposed a repeated multiscale morphology to deal with surplus noise at some small scales after conventional multiscale analysis. Refs [101,102] defined the SE scales from unit scale to 0.6 times impulse period when extracting bearing fault feature frequencies. Gong et al. [103] introduced an iterative asymmetric multiscale morphology targeted at the amplitude demodulation of vibration signatures of defective bearings.

Based on the MSM theory in Section 2.3.2, it can be noticed that this method uses a series of scales to perform morphological processing, thus the last scale is defined properly. To the Refs [98–103], the problem is solved by the experimental way. In fact, according to the morphological filtering characteristic, the scale or length of SE is not bigger than the repetitive cycle of rotating parts fault, thus Li et al. [104] proposed the scale as f_s/f -2, where f_s is the sampling frequency of bearing vibration signals, and f is bearing fault feature frequencies. The same method is found in Refs [105–108].

Although the last scale of structuring element is obtained by math computation based on sampling rate and rotating feature frequency, the MSM methods still lack certain adaptation. In order to handle the problem, Zhang et al. [109] employed an adaptive local-peak algorithm to define the length and height scales. Li et al. [110] combined Zhang's study with bandwidth empirical mode decomposition to detect bearing characteristic frequency and its harmonic, and Patel et al. [111] melted Zhang's work with adaptive noise cancellation to improve bearing defect detection. Shuai et al. [112] designed based on local-peak-interval scale definition with support vector regression to distinguish roller bearing fault types. Cui et al. [113] presented information-entropy threshold to obtain optimal scales. Shen et al. [114] and Li et al. [115] developed a bearing fault detection method termed time-varying-scale, in which all flat-SE length scales are given by the time distance between two adjacent impulse peaks in local range. Deng et al. [116] studied particle swarm method to optimize the weight of each scale in the reconstructed signals, and finally roller bearing fault diagnosis effect is improved. Yan et al. [117] presented a scale definition method based on bearing feature frequencies.

Note that the MSM studies above all use a SE with one defined scale to perform time-shifting morphological operation into an original signal, until all SEs are used. Differently, Wang et al. [118,119] proposed a novel structuring element scale definition in more microcosmic way, in which the shape and length of SE is specified based on local minima in the two adjacent waveforms of the raw signals. What's more, such SE will conduct morphological operation just in local area, without the time-shifting operation in the whole signal and without signal reconstruction by the results of all SEs. In other words, one SE is defined and operated in local area. When it is completed in this area, another new one is used in the same way. Although it is completely different from the conventional

 doi:10.20944/preprints202512.0987.v1

multiscale analysis, structural elements are varied and the model is grouped into the multiscale morphology.

3.2.2. MSM to Detect Gear Defect

Li et al. [120] explored multiscale morphology analysis combined with empirical mode decomposition to identify the seeded wear faults on sun, planet and ring gears. Li et al. [121] investigated the multiscale filtering capacity of eight morphological operators, and found that it surpasses continuous wavelet transform in extracting gear feature characteristics. Guo et al. [122] defined the flat SE scales into a certain range decided by the signal sampling frequency and gear fault feature frequency, then used the multiscale morphological method to diagnose sun gear chipping in a planet gearbox. Wang et al. [123] utilized three fixed scales to diagnose the gearbox faults, Facing gearbox defect recognizing, Cai et al. [124] similarly defined the SE scales the is the same as Ref [104].

To the flexible definition of the SE scales, Refs [125–127] integrated the adaptive scale definition method in Ref [109] with other approaches to discriminate gearbox faults. Zhang et al. [128] and Yu et al. [129] developed a multiscale morphology to diagnose gear fault, where the SE scales are chose adaptively based on kurtosis. Liu et al. [130] developed a scale optimization method based on the parameter changing of impact signals to locate gear faults. Yan et al. [131] constructed a special indictor melting signal-to-noise ratio with fault feature ration to choose the SE scales when identifying wind turbine gearbox faults. Liu et al. [132] considered Chebyshev window as structuring elements, and defined the length and height scales based on the signal features of planetary gearbox. Zhuang et al. [133] proposed the back-propagation learning algorithm to update the SE scale for detecting gearbox failure. In order to remove impulse interference of the vibration signals of gearbox, Cao et al. [134] designed the SE length selection based on max maximizing L-kurtosis.

3.3. Morphological Pattern Spectrum-Based Rotating Parts Fault Diagnosis

Different to SSM and MSM, MPS construct a one-to-one mapping relationship between the quantifiable spectrum index and the defined pattern, it is able to distinguish rotating parts working statue under different working conditions.

3.3.1. MPS to Detect Bearing Defect

Chen et al. [135] calculated morphological pattern spectrum with double-dot SEs, and used an improved support vector machine (SVM) algorithm to classify the outer fault, the inner race fault, and the ball fault on rolling ball bearing. In order to improve bearing fault classification accuracy, Gao et al. [136] proposed an optimized method based on MSP and S transform to bearing faults, and found that it can successfully distinguish normal state and abnormal state with three fault levels. Sun et al. [137] calculated morphological pattern spectrum obtained by dilation, with support vector machine to classify bearing faults. Zhu et al. [138] noticed that in a signal from bearing fault the detailed information is similar but the position is different, thus introduced the feature vector of hit and miss at local impact feature position to enhance classifier recognition performance. Li et al. [139] found that MPS is obtained by using the difference between open minus close, and least square support vector machine to recognize different wheelset bearing fault types. Gao et al. [140] developed the MPS of the time-frequency representations of signal as the input feature vectors of the classifier to identify bearing states.

Those investigations mentioned above are applications on basic MPS. In fact, pattern spectrum can be further developed to special target. Hao et al. [141,142] believed that the combination between morphological pattern spectrum entropy and barycenter scale location of spectrum is more effective than the combination between kurtosis and enveloping demodulating spectrum when differentiating six bearing defects. Wang et al. [143] noticed that original MPS cannot recognize damaged and normal bearings, and then developed the sample entropy and Lempel-Ziv complexity of MPS curve as bearing fault classification index. Yan et al. [144] exploited multiscale pattern gradient spectrum

 doi:10.20944/preprints202512.0987.v1

entropy based on MSP as the input feature sets of extreme machine learning, and the bearing defect classification demonstrated the effectiveness of this combined approach. Yu et al. [145] developed MPS entropy and pattern spectrum values as the bearing feature parameters of proximal SVM.

MPS is utilized as not only bearing fault classification tool, but also bearing performance estimation indicator. For instance, Zhao et al. [146,147] presented a new idea entitled high-order differential morphological spectrum entropy based on MPS and performed it on bearing performance trend prediction. Li et al. [148] extended the conventional definition of MSP to the general space, and simulation and practical applications demonstrated that the improvement is capable of evaluating bearing performance. Gao et al. [149] studied the relationship between generalized pattern spectrum entropy and performance degradation course, showing that they have a good correlation. Similarly, Wang et al. [150] found that it is accordant and preferable for the relevance between improved pattern spectrum entropy and bearing degradation degree.

3.3.2. MPS to Detect Gear Defect

Li et al. [151] constructed morphological pattern spectra obtained by separately using four basic operators as the input of K nearest neighbor classifier, Bayes classifier and least-square support vector machine, and finally observed that the MPS obtained by erosion are best for gear fault classification. Li et al. [152] characterized the time-frequency representation based on S transform by morphological pattern spectrum to recognize five gear states in a gearbox. Barbieri [153] considered a correlation analysis according to two pattern spectra produced by signals with and without gear fault, and integrated it with wavelet transform, single value decomposition, and stabilization diagram to discriminate the defects of gear and bearing installed in gearbox.

3.4. Morphological Wavelet -Based Rotating Parts Fault Diagnosis

Morphological wavelet is a nonlinear multiresolution signal decomposition scheme, with high computation efficiency and retaining local features of signal. It is capable of providing a different view to rotating part detect diagnosis.

3.4.1. MW to Detect Bearing Defect

Hao and Chu [154] discussed a morphological undecimated wavelet decomposition, keeping the length of original signals and showing the less distortion in time-domain signal, and the actual bearing defects applications indicated that this method well extract impulses. Wang et al. [155] designed a mixed scheme based on lifting morphological wavelet and ensemble empirical mode composition for extracting fault features of defective rolling element bearings. Li et al. [156] proposed an adaptive morphological gradient lifting wavelet, in which the average filter and morphological gradient filter are used to update the approximating signal, and the results showed that the proposed algorithm outperforms linear wavelet transform in bearing fault diagnosis. Li et al. [157] analyzed the geometrical structures of the bearing vibrations dispersed various morphological scales, and developed morphological stationary wavelet to extract bearing fault features. Chen et al. [158] performed a MW decomposition method based on open and closing operators for impulse feature extraction of damaged bearings.

Han et al. [159] carried out morphological wavelet and least squares support vector machine to classify the various type of bearing failure. Meng et al. [160] used morphological wavelet and morphological filter to diagnose the outer, inner, rolling ball and mixed bearing faults. Khakipour et al. [161] performed morphological wavelet based on morphology gradient operator to detect bearing flaws and proved its superiority by comparing with morphological harr wavelet and the morphological undecimated wavelet decomposition. Li et al. [162] focused their study in using undecimated MW lifting scheme based on morphological convolution operator to identify bearing defects. Guo et al. [163] presented a combined scheme based on morphological undecimated wavelet and morphological filtering to extract the weak fault feature of rolling bearing. Li et al. [164] used the

 doi:10.20944/preprints202512.0987.v1

different morphology operators in morphology undecimated wavelet to well suppress noisy signals, and the results indicated that it diagnoses the wheelset bearing compound faults accurately.

Li et al. [165] took full advantage of the nonlinear characteristics of morphology Harr wavelet, and combined it with Perona-Malik filtering for detect the bearing inner race failure. Duan et al. [166] exploited an empirical morphology undecimated wavelet to process the faulty bearing vibration signals, and found that it effectively detect the fault with high computation efficiency. In addition, Wang et al. [167] presented a morphology undecimated wavelet scheme, in which an improved gradient based on closing and opening is considered as analysis operator, and showed that the improvement can avoid statistic bias in bearing fault vibrations.

Zhang et al. [168] proposed the combination between dilation and erosion as and one between opening and closing superlatively as synthesis operator and analysis operator, and the results demonstrated that the undecimated decomposition is suited for bearing faults diagnosis. Lin et al. [169] constructed morphological wavelet package decomposition method, and at the same time set soft threshold to remove the noisy signals for bearing fault feature detection. Yang et al. [170] presented an integrated method based on morphology wavelet and S transform, demonstrating that MW can inhibit noise and the harmonic components of axis rotating frequency to bearing fault classification.

3.4.2. MW to Detect Gear Defect

Li et al. [171] utilized morphological gradient wavelet to detect gear fault feature frequencies. Zhang et al. [172] presented multi-scale morphological undecimated wavelet decomposition and grey incidence to identify the gear fault patterns. Hong et al. [173] employed morphological mean wavelet transform to gear fault diagnosis and found that it has the sensitivity to local extrema of signal and the high effectiveness to reduce noise. Zhang et al. [174] developed morphological Harr wavelet to deal with original signals and used permutation entropy as the fault eigenvalue for detecting various gear fault types. Cai et.al [175] proposed a morphological wavelet method to cancel the strong noisy signals when diagnosing a gear fault. Ding et al [176] introduced morphological Harr wavelet to purify the vibration signals of faulty gearbox and used Permutation entropy to classify fault type. Zhang et al. [177] developed max-lifting morphological wavelet for extracting gear features, in which dilation is used as predicted and updated operator.

Tong et al. [178] employed weighted morphological un-decimated wavelet decomposition and correlated kurtosis to gear defects, using difference morphological gradient operator based on opening and closing. Shen et al. [179] found that morphological wavelet de-noising provide good behavior in gear fault features. Li et al. [180] believed that the traditional MW is disadvantage in dealing with sudden impulses of damage gear because of using a fixed filter, and proposed adaptive morphological undated lifting wavelet.

Table 1. Summarization of rotating components using the morphology-based method.

Object	Ref.	Method
Bearing	Nakolaou [74], Dong [75], Chen [76], Chao [77], He [78], Meng [79]，Yu [80], Hu [81], Hu [82], Wang [83], Jia [84], Van [85], Dong [86], Raj [87], Zhang [88], Osman [89], Lv [90], Li [91.92]	SSM
	Li [98], Feng [99], Gong [100], Lv [101], Tang [102], Gong [103], Li [104], Yan [105], Qu [106], Yu [107], Li [108], Zhang [109], Li [110], Patel [111], Shuai [112], Cui [113], Shen [114], Li [115], Deng [116], Yan [117], Wang [118,119]	MSM
	Chen [135], Gao [136], Sun [137], Zhu [138], Li [139], Gao [140], Hao [141,142], Wang [143], Yu [144], Yan [145], Zhao [146,147], Li [148], Gao [149], Wang [150]	MPS

 doi:10.20944/preprints202512.0987.v1

	Hao [154], Wang [155], Li [156], Li [157], Chen [158], Han [159], Meng [160], Khakipour [161], Li [162], Guo [163], Li [164], Li [165], Duan [166], Wang [167], Zhang [168], Lin [169], Yan [170]	MW
Gear	Feng [93], Chen [94], Gryllias [95], Lin [96], Guo [97]	SSM
	Li [120], Li [121], Guo [122], Wang [123], Cai [124], Li [125], Yu [126], Luo [127], Zhang [128], Yu [129], Liu [130], Yan [131], Liu [132], Zhuang [133], Cao[134]	MSM
	Li [151], Li [152], Barbieri [153]	MPS
	Li [171], Zhang [172], Hong [173], Zhang [174], Cai [175], Ding [176], Zhang [177], Tong [178], Shen [179], Li [180]	MW
Others	Li [181], Jiang [182]	MSM
	Li [183]	MPS

3.5. Morphology-Based Methods to Other Mechanical Defective Objects

Li et al. [181] investigated adaptive multiscale morphology to recognize railway wheel flat, where the optimal scales are defined by spectrum kurtosis crooner criterion. Jiang et al. [182] studied local mean decomposition and adaptive multiscale morphology to demodulate the defective hydraulic pump signals and believed that the combined method is anti-noise and has stronger demodulation ability. Li et al. [183] introduced an improved morphology pattern spectrum into time-frequency analysis and the results illustrated that this approach is effective to characterize the vibration signals of engine with five working states.

3.6. Comparison and Analysis of Operators and SE in Applications

Through these representative applications, which are listed in Table 1 to present a more direct view for interested readers, it shows that mathematical morphology is applicable and robust in the rotating machine fault diagnosis area. Meanwhile, it is also noticed that these studies concentrate two aspects: morphological operator and structuring element, which benefit enhancing the morphology performance in practical applications. As a result, morphological operator selection and structuring element definition are further analyzed here.

3.6.1. Morphology Operator Analysis

Morphological operator selection, relatively speaking, is handled easily. Apparently, basic operators have individual behavior to signal morphological feature recognition, for example, closing operator can capture positive impulses and restrain negative ones. Meanwhile, basic operators can constitute various combined morphological gradients, providing more choices for actual applications.

In general, if it focuses on the extracting morphological feature in time-domain, closing and opening, and the combination between them are a better candidate, because they possess the recovery capacity to an original signal. When an application pays attention to isolating frequency-domain feature components, gradient operator should be considered because they are able to retain positive and negative feature components in a signal, with lesser loss to them. In some special cases, more complex combination patterns between basic operators, such as product, convolution and cross-correlation, are utilized for attain superior result [184]. Hence, the selectable candidates are relatively limited in actual application, i.e., basic and gradients operators.

3.6.2. Structuring Element Analysis

To a structuring element, the first should be considered is shape. In general, the shape almost has no effect to process a 1D signal, e.g., a vibration signal sampled from rotating machine. The reason is space dimension mismatching between structuring element and signal. In order to explain the problem, a diamond-shaped SE presented in Figure 4 is considered, in which black dot and gray dot

 doi:10.20944/preprints202512.0987.v1

represent 1 and 0 respectively, and the black one circled by a red rectangle is the origin. Let a 1D signal be $\{x_0, x_1, \ldots, x_i, \ldots, x_{n-1}, x_n\}$. When the point x_i is processed and firstly overlapped with the origin, other data points covered by the neighborhoods are detected. Obviously, these points only at the left and right sides of x_i can be introduced into the morphological operation, because there are no others at the top and bottom area of x_i. It means that when the diamond SE is used, just the black dots linked by a blue line in Figure 5 work as effective neighborhood to the 1D signal and will control the morphological computation range. Accordingly, the complex shape has on influence to morphological processing of one-dimensional signal. Here, it must be emphasized that the shape has no effect to the morphological result, just when structural element is flat. On the contrary, if the SE is non-flat, its length and height together construct a specified figure, such as triangle SE and Gaussian SE, now the height parameter is introduced in morphological, thus such shape will affect the morphological result.

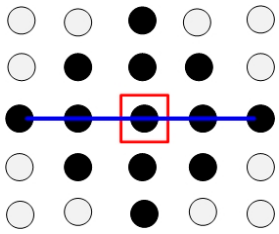

Figure 5. Dimond structuring element.

Furthermore, as mentioned above, once the SE height is considered, their specified values will take part in a morphology computation, i.e., the length and height parameters work together to the morphology result. However, it can be noticed that in the aforementioned morphology applications the overwhelming cases use only the length parameter, and a few cases [109–111,125–127] use the two parameters together. This is mainly because most cases just concern the nonlinear filtering of mathematical morphology, that is, using the length controls the filtering range, thereby obtaining a good filtering performance. In addition, the SE length describes the time-scale representation for feature information like their cycle of rotating part faults, only if the inputting speeds and the mechanical structure configuration are determined, it can be exactly and easily achieved by theoretical calculation. However, the SE height corresponds to a spatial representation to a signal with apparent randomness. Therefore, it is more difficult to define the height than to define the length, and non-flat SE is less utilized in the mechanical fault diagnosis field.

On the other hand, the essence of morphology theory is the geometrical structure interacting and matching between SE and a processed object. In this situation, if the length is only considered, the flat SE and the object lack higher spatial matching. Obviously, a better way should use non-flat SE, in the sense that such morphology application can take full advantage of two merits: non-linear filtering and closer shape mapping between the two objects. If so, much more characteristic information could be extracted. Certainly, the key is that how to determine the length and height of structuring element. Although a few tries are conducted, it still needs further study.

4. Discussion and Development Orientation

Under the framework of mathematical morphology, four methods are introduced and their relevant applications on detecting rotating machine flaws are presented in this study. As an open study topic, there still are several unsolved problems and potential developments in mathematical morphology:

(1) when single- and multi-scale analysis use SE, especially large-scale ones, the morphological processing easily suffer from edge distortion in time domain following the shift of SE. Essentially speaking, it is determined by the nonlinear filtering mechanism, i.e., local extrema search. So,

 doi:10.20944/preprints202512.0987.v1

considering from signal restoring in time domain with retaining this nonlinear filtering character, how to alleviate the time-domain distortion as much as possible should be further studied.

(2) In morphology theory, the core is how to construct the structure element adaptively. It can be known that once the scales are defined, they will not change in one morphological operation. However, dynamic characteristics of a real signal always change following sampling time. Obviously, the localized variability of SE is a good ability that relieves the dependence to the scale constraint, highlight the dynamic characteristics of signal, and enhance the feature extracting capacity.

(3) One of the advantages of morphology is low computation cost, and it is very essential to real-time monitoring of mechanical equipment. Notice that Morphology processing is conducted by using the point-wise shift of SE inside original signal, sometimes the shifting is maybe unnecessary to such processing, at least in specific range, for example the interval between two impulses produced by rotating part faults. In a permissible condition without the loss in time- or frequency domain, the non-pointwise shift could be considered, and it will further improve the morphology computation efficiency.

(4) Morphology pattern spectrum is a fault classification tool. In actual applications, noise disturbance will affect this processing accuracy, thus in some cases MPS frequently works with other pattern classification algorithms to improve the classification performance. On the other aspect, MPS can be regarded as the moment of first-order of a distribution function. It is evident that there exist the different high order moments between feature shapes and noise in a signal. Based on such consideration, it can inhibit the noise interference to strengthen feature shape classification performance.

(5) Nonlinear multiresolution morphological wavelet is sensitive to certain types of noise, developing more robust methods that are specifically designed to mitigate the impact of noise could enhance the reliability of morphological wavelet-based fault detection. This could involve new mathematical formulations or filtering techniques that preserve important nonlinear features while suppressing noise.

(6) Morphology processing is conducted by one computation in SMS and MPS and multi-computations in MSM and MW, but they are unrelated each other, thus the current morphology-based approaches rely on the defined SE highly. If a novel morphological computation model can be figured out, the dependence to SE can be reduced in a certain degree. For instance, the gradient descent algorithm in optimization theory is to gradually obtain the optimal solution. Maybe, it is a good reference to mathematical morphology.

5. Concluding Remarks

A literature surveys and summarization on mathematical morphology and actual applications for rotating machine fault diagnosis is presented in this paper. Section 2 describes two basic elements, structuring element and morphology operators, and four morphology-based methods, containing single-scale morphology, multi-scale morphology, morphological pattern spectrum and morphological wavelet. Their typical applications on rotating machine fault diagnosis and classification are given with a clear classification as fault object and diagnostic method, and the effect of operator and SE to morphology result is analyzed in Section 3. Finally, several potential research directions are proposed. The review paper attempts to introduce diagnosing methods based on mathematical morphology as much as possible and summarize the related applications in the rotatory machine fault detection field. It is believed that it can offer a comprehensive reference to researchers who are interested to rotating machine fault diagnosis based on mathematical morphology.

Author Contributions: Conceptualization, methodology, writing-original draft, Tingkai Gong; Writing-review & editing, supervision, Xiaohui Yuan and Zhilong Li; Literature investigation and formal analysis, Bin Ji. All authors have read and agreed to the published version of the manuscript.

 doi:10.20944/preprints202512.0987.v1

Conflicts of Interest: The authors declare that they have no known competing financial interests or personal relationships that could have appeared to influence the work reported in this paper.

References

1. Jardine, A. K. S.; Lin, D.; Banjevic, D. A Review on Machinery Diagnostics and Prognostics Implementing Condition-Based Maintenance. *Mech. Syst. Signal Proc* **2006**, *20*, 1483–1510. [CrossRef]
2. Wei; Li; Xu; Huang. A Review of Early Fault Diagnosis Approaches and Their Applications in Rotating Machinery. *Entropy* **2019,** *21* , 409. [CrossRef]
3. Griffin, D.; Jae Lim. Signal Estimation from Modified Short-Time Fourier Transform. *IEEE Trans. Acoust. Speech Signal Process* **1984**, *32* , 236–243.[CrossRef]
4. Durak, L.; Arikan, O. Short-Time Fourier Transform: Two Fundamental Properties and an Optimal Implementation. *IEEE Trans. Signal Process* **2003**, *51* , 1231–1242. [CrossRef]
5. Sun, R.-B.; Yang, Z.; Chen, X.; Tian, S.; Xie, Y. Gear Fault Diagnosis Based on the Structured Sparsity Time-Frequency Analysis. *Mech. Syst. Signal Proc.* **2018**, *102*, 346–363. [CrossRef]
6. Liu, H.; Li, L.; Ma, J. Rolling Bearing Fault Diagnosis Based on STFT-Deep Learning and Sound Signals. *Shock Vib* **2016**, *2016*, 1–12.[CrossRef]
7. Tao, H.; Wang, P.; Chen, Y.; Stojanovic, V.; Yang, H. An Unsupervised Fault Diagnosis Method for Rolling Bearing Using STFT and Generative Neural Networks. *J. Frankl* **2020**, *357*, 7286–7307. [CrossRef]
8. Yan, R.; Gao, R. X.; Chen, X. Wavelets for Fault Diagnosis of Rotary Machines: A Review with Applications. *Signal Process* **2014**, *96*, 1–15. [CrossRef]
9. Yuan, J.; Yao, Z.; Zhao, Q.; Xu, Y.; Li, C.; Jiang, H. Dual-Core Denoised Synchrosqueezing Wavelet Transform for Gear Fault Detection. *IEEE Trans. Instrum. Meas* **2021**, *70*, 1–11. [CrossRef]
10. Fan, X.; Zuo, M. J. Gearbox Fault Detection Using Hilbert and Wavelet Packet Transform. *Mech. Syst. Signal Proc* **2006**, *20* , 966–982. [CrossRef]
11. Sung, C. K.; Tai, H. M.; Chen, C. W. Locating Defects of a Gear System by the Technique of Wavelet Transform. *Mech. Mach. Theory* **2000**, *35* , 1169–1182. [CrossRef]
12. Shao, H.; Jiang, H.; Wang, F.; Wang, Y. Rolling Bearing Fault Diagnosis Using Adaptive Deep Belief Network with Dual-Tree Complex Wavelet Packet. *ISA Trans* **2017**, *69*, 187–201. [CrossRef]
13. Yu, D.; Cheng, J.; Yang, Y. Application of EMD Method and Hilbert Spectrum to the Fault Diagnosis of Roller Bearings. *Mechanical Systems and Signal Processing* **2005**, *19* , 259–270. [CrossRef]
14. Yu, Y.; YuDejie; Junsheng, C. A Roller Bearing Fault Diagnosis Method Based on EMD Energy Entropy and ANN. *Mech. Syst. Signal Proc* **2006**, *294* , 269–277. [CrossRef]
15. Gong, X.; Ding, L.; Du, W.; Wang, H. Gear Fault Diagnosis Using Dual Channel Data Fusion and EEMD Method. J. *Sound Vib* **2017**, *174*, 918–926. [CrossRef]
16. Wang, X.; Liu, C.; Bi, F.; Bi, X.; Shao, K. Fault Diagnosis of Diesel Engine Based on Adaptive Wavelet Packets and EEMD-Fractal Dimension. *Mech. Syst. Signal Proc* **2013**, *41* , 581–597. [CrossRef]
17. Fu, Q.; Jing, B.; He, P.; Si, S.; Wang, Y. Fault Feature Selection and Diagnosis of Rolling Bearings Based on EEMD and Optimized Elman_AdaBoost Algorithm. *IEEE Sen. J* **2018**, *18* , 5024–5034. [CrossRef]
18. Dragomiretskiy, K.; Zosso, D. Variational Mode Decomposition. *IEEE Trans. Signal Process* **2014**, *62* , 531–544.[CrossRef]
19. Gong, T.; Yuan, X.; Yuan, Y.; Lei, X.; Wang, X. Application of Tentative Variational Mode Decomposition in Fault Feature Detection of Rolling Element Bearing. *Measurement* **2018**, *135*, 481–492. [CrossRef]
20. Liu, C.; Cheng, G.; Chen, X.; Pang, Y. Planetary Gears Feature Extraction and Fault Diagnosis Method Based on VMD and CNN. *Sensors* **2018**, *18*, 1523. [CrossRef]
21. Li, H.; Liu, T.; Wu, X.; Chen, Q. An Optimized VMD Method and Its Applications in Bearing Fault Diagnosis. *Measurement* **2020**, *166*, 108185. [CrossRef]
22. Zhou, J.; Xiao, M.; Niu, Y.; Ji, G. Rolling Bearing Fault Diagnosis Based on WGWOA-VMD-SVM. *Sensors* **2022**, *22* , 6281–6281. [CrossRef]
23. Wang, Y.; Markert, R. Filter Bank Property of Variational Mode Decomposition and Its Applications. *Signal Process* **2016**, *120*, 509–521. [CrossRef]
24. Serra, J. Introduction to Mathematical Morphology. *Graph. Models* **1986**, *35*, 283–305. [CrossRef]

 doi:10.20944/preprints202512.0987.v1

25. Haralick, R. M.; Sternberg, S. R.; Zhuang, X. Image Analysis Using Mathematical Morphology. *IEEE Trans. Pattern Anal. Mach. Intell.* **1987**, *PAMI-9*, 532–550. [CrossRef]
26. Image Analysis and Mathematical Morphology. *Computer Graphics and Image Processing* **1982**, *20* , 96–97. [CrossRef]
27. Zana, F.; Klein, J.-C. . Segmentation of Vessel-like Patterns Using Mathematical Morphology and Curvature Evaluation. *IEEE Trans. Image Process* **2001**, *10* , 1010–1019. [CrossRef]
28. Shih, H.-C.; Liu, E.-R. Automatic Reference Color Selection for Adaptive Mathematical Morphology and Application in Image Segmentation. *IEEE Trans. Image Process* **2016**, *25* , 4665–4676. [CrossRef]
29. Bouchet, A.; Montes, S.; Ballarin, V.; Díaz, I. Intuitionistic Fuzzy Set and Fuzzy Mathematical Morphology Applied to Color Leukocytes Segmentation. *Signal Image Video Process* **2019**, *14* , 557–564. [CrossRef]
30. Vincent, L.; Dougherty, E.R. Morphological Segmentation for Textures and Particles. In *Digital image processing methods*; CRC Press, 2020; pp. 43–102.[CrossRef]
31. Wu, Y.; Li, Q. The Algorithm of Watershed Color Image Segmentation Based on Morphological Gradient. *Sensors* **2022**, *22*, 8202. [CrossRef]
32. Chatterjee, S.; Dey, D.; Munshi, S. Mathematical Morphology Aided Shape, Texture and Colour Feature Extraction from Skin Lesion for Identification of Malignant Melanoma. In *2015 International Conference on Condition Assessment Techniques in Electrical Systems (CATCON)*; 2015; pp. 200–203.[CrossRef]
33. Godse, R.; Bhat, S. Mathematical Morphology-Based Feature-Extraction Technique for Detection and Classification of Faults on Power Transmission Line. *IEEE Access* **2020**, *8*, 38459–38471. [CrossRef]
34. Xiong, W.; Zhou, L.; Yue, L.; Li, L.; Wang, S. An Enhanced Binarization Framework for Degraded Historical Document Images. *EURASIP J. Image Video Process* **2021**, *2021* . [CrossRef]
35. Kimori, Y. Mathematical Morphology-Based Approach to the Enhancement of Morphological Features in Medical Images. *J. Clin. Bioinform* **2011**, *1* , 33. [CrossRef]
36. Moslem Ouled Sghaier; Foucher, S.; Lepage, R. River Extraction from High-Resolution SAR Images Combining a Structural Feature Set and Mathematical Morphology. *IEEE J. Sel. Top. Appl. Earth Observ. Remote Sens* **2017**, *10* , 1025–1038. [CrossRef]
37. Gavankar, N. L.; Ghosh, S. K. Automatic Building Footprint Extraction from High-Resolution Satellite Image Using Mathematical Morphology. *Eur. J. Remote Sens* **2017**, *51* , 182–193. [CrossRef]
38. Ma, X.; Liu, S.; Hu, S.; Geng, P.; Liu, M.; Zhao, J. SAR Image Edge Detection via Sparse Representation. *Soft Computing* **2017**, *22* , 2507–2515. [CrossRef]
39. Pei, Y.; Liu, C.; Lou, R. Multi-Scale Edge Detection Method for Potential Field Data Based on Two-Dimensional Variation Mode Decomposition and Mathematical Morphology. *IEEE Access* **2020**, *8*, 161138–161156. [CrossRef]
40. Zhao, Y.; Gui, W.; Chen, Z.; Tang, J.; Li, L. Medical Images Edge Detection Based on Mathematical Morphology. *IEEE Annual; Santa Barbara* **2005,** 6492-6495. [CrossRef]
41. Huang, C.P.; Wang, R.Z. An Integrated Edge Detection Method Using Mathematical Morphology. *Pattern Recogn, Image Anal.* **2006**, *16*, 406–412. [CrossRef]
42. Xu, M. K.; Ping, X. J.; Li, T. Y. A New Time-Frequency Spectrogram Analysis of FH Signals by Image Enhancement and Mathematical Morphology. In *Fourth Int. Conf. Image and Graph*; Chengdu, China, **2007**; pp 610−615. [CrossRef]
43. Román, J. C. M.; Fretes, V. R.; Adorno, C. G.; Silva, R. G.; Noguera, J. L. V.; Legal-Ayala, H.; Mello-Román, J. D.; Torres, R. D. E.; Facon, J. Panoramic Dental Radiography Image Enhancement Using Multiscale Mathematical Morphology. *Sensors* **2021**, *21*, 3110. [CrossRef]
44. Maragos, P.; Pessoa, L. F. Morphological Filtering for Image Enhancement and Detection. In *The Image and Video Process Handbook*; **1999**; pp 135−156.
45. Kimori, Y. Morphological Image Processing for Quantitative Shape Analysis of Biomedical Structures: Effective Contrast Enhancement. *J. Synchrot. Radiat.* **2013**, *20*, 848–853. [CrossRef]
46. Li, Q.; Qi, Y.-S.; Gao, X.-J.; Li, Y.-T.; Liu, L.-Q. A Signal Based "W" Structural Elements for Multi-Scale Mathematical Morphology Analysis and Application to Fault Diagnosis of Rolling Bearings of Wind Turbines. *Int. J. Autom. Comput.* **2021**, *18*, 993–1006. [CrossRef]

 doi:10.20944/preprints202512.0987.v1

47. Hu, A. J.; Tang, G. J.; An, L. S. New Method of Removing Pulsed Noises in Vibration Data. J. Vib. Shock. **2006**, 25, 126–129.
48. Zhang, W.; Zhou, X.; Lin, Y. Application of Morphological Filter in Pulse Noise Removing of Vibration Signal. In *Cong. Image Signal Process.*; Sanya, China, **2008**; pp 132–135.
49. Maragos, P. Pattern Spectrum and Multiscale Shape Representation. *IEEE Trans. Pattern Anal. Mach. Intell.***1989**, *11*, 701–716. [CrossRef]
50. Georges Matheron. *Random Sets and Integral Geometry*; John Wiley & Sons, **1974**.
51. Dornaika, F.; Zhang, H. Granulometry Using Mathematical Morphology and Motion. In *Proc. IAPR Machine Vision Appl.*; Tokyo, Japan, **2000**; pp 51–54.
52. Maria, V.; Vitria, J. M. Mathematical Morphology, Granulometries, and Texture Perception. In *Proc. SPIE Conf. Image Algebr. Morphological Image Process. IV*; San Diego, USA, **1993**; pp 152–161. [CrossRef]
53. Laurent, N.; Talbot, H. *Mathematical Morphology: From Theory to Applications*; John Wiley & Sons: Hoboken, USA, **2013**.
54. Serra, J.; Soille, P. *Mathematical Morphology and Its Applications to Image Processing*; Springer Science & Business Media, **2012**.
55. Pei, S.-C. Subband Decomposition of Monochrome and Color Images by Mathematical Morphology. *Opt. Eng.* **1991**, *30*, 921. [CrossRef]
56. Pei, S.-C.; Chen, F.-C. Hierarchical Image Representation by Mathematical Morphology Subband Decomposition. *Pattern Recognit. Lett.* **1995**, *16*, 183–192. [CrossRef]
57. Egger, O.; Li, W. Very Low Bit Rate Image Coding Using Morphological Operators and Adaptive Decompositions. In *Proc. Int. Conf. on Image Process.*; Tustin, USA, **1994**; pp 326–330. [CrossRef]
58. Florêncio, D. A. F.; Schafer, R. W. A Non-Expansive Pyramidal Morphological Image Coder. In *Proc. Int. Conf. Image Process.*; Austin, USA, **1994**; pp 331–335. [CrossRef]
59. de Queiroz, R. L.; Florencio, D. A. F.; Schafer, R. W. Nonexpansive Pyramid for Image Coding Using a Nonlinear Filterbank. *IEEE Trans. Image Process.* **1998**, *7*, 246–252. [CrossRef]
60. Cha, H.; Luis, F. C. Adaptive Morphological Representation of Signals: Polynomial and Wavelet Methods. *Multidimens. Syst. Signal Process.* **1997**, 8, 249–271. [CrossRef]
61. Wim Sweldens. The Lifting Scheme: A Construction of Second Generation Wavelets. *SIAM J. Math. Anal.* **1998**, *29*, 511–546. [CrossRef]
62. Sweldens, W. The Lifting Scheme: A Custom-Design Construction of Biorthogonal Wavelets. *Appl. Comput. Harmon. Anal.* **1996**, *3* , 186–200. [CrossRef]
63. Sweldens, W. Lifting Scheme: A New Philosophy in Biorthogonal Wavelet Constructions. In *Wavelet Appl. Signal Image Processing III*; San Diego, USA, **1995**; pp 68–79.
64. Claypoole, R. L.; Davis, G. M.; Sweldens, W.; Baraniuk, R. Nonlinear Wavelet Transforms for Image Coding. In *Conference Record of the Thirty-First Asilomar Conference on Signals, Systems and Computers*; Pacific Grove, USA, **1997**; pp 662–667. [CrossRef]
65. Claypoole, R. L.; Baraniuk, R. G.; Nowak, R. D. Lifting Construction of Non-Linear Wavelet Transforms. In *Proc. IEEE-SP Int. Symp. Time-Frequency Time-Scale Anal.*; Pittsburgh, USA, **1998**; pp 49–52. [CrossRef]
66. Claypoole, R. L.; Baraniuk, R. G.; Nowak, R. D. Adaptive Wavelet Transforms via Lifting. In *Proc. IEEE Int. Conf. Acoust, Speech Signal Process.*; Seattle, USA, **1999**; pp 1513–1516.
67. Wang, X.; Liang, J.; Wang, M. On-Line Fast Palmprint Identification Based on Adaptive Lifting Wavelet Scheme. *Knowledge-Based Syst.* **2013**, *42*, 68–73. [CrossRef]
68. Heijmans, H. J. A. M.; Pesquet-Popescu, B.; Piella, G. Building Nonredundant Adaptive Wavelets by Update Lifting. *Appl. Comput. Harmon. Anal.* **2005**, *18*, 252–281. [CrossRef]
69. Piella, G.; Heijmans, H. J. A. M. Adaptive Lifting Schemes with Perfect Reconstruction. *IEEE Trans. Signal Process.* **2002**, *50*, 1620–1630. [CrossRef]
70. Piella, G.; Pesquet-Popescu, B.; Heijmans, H. Adaptive Update Lifting with a Decision Rule Based on Derivative Filters. *IEEE Signal Process. Lett.* **2002**, *9* , 329–332. [CrossRef]
71. Piella, G.; Pesquet-Popescu, B.; Heijmans, H. J. A. M. Gradient-Driven Update Lifting for Adaptive Wavelets. *Signal Process. Image Commun.* **2005**, *20*, 813–831. [CrossRef]

 doi:10.20944/preprints202512.0987.v1

72. Heijmans, H. J. A. M.; Goutsias, J. Nonlinear Multiresolution Signal Decomposition Schemes. II. Morphological Wavelets. *IEEE Trans. Image Process.* **2000**, *9*, 1897–1913. [CrossRef]
73. Goutsias, J.; Heijmans, H. J. A. M. Nonlinear Multiresolution Signal Decomposition Schemes. I. Morphological Pyramids. *IEEE Trans. Image Process.* **2000**, *9*, 1862–1876. [CrossRef]
74. NIKOLAOU, N. G.; ANTONIADIS, I. A. APPLICATION of MORPHOLOGICAL OPERATORS as ENVELOPE EXTRACTORS for IMPULSIVE-TYPE PERIODIC SIGNALS. *Mech. Syst. Signal Proc.***2003**, *17*, 1147–1162. [CrossRef]
75. Dong, S.; Tang, B.; Zhang, Y. A Repeated Single-Channel Mechanical Signal Blind Separation Method Based on Morphological Filtering and Singular Value Decomposition. *Measurement* **2012**, *45*, 2052–2063. [CrossRef]
76. Chen, X.; Liu, X.; Dong, S.; Liu, J. Single-Channel Bearing Vibration Signal Blind Source Separation Method Based on Morphological Filter and Optimal Matching Pursuit (MP) Algorithm. *J. Vib.* Control. **2013**, *21*, 1757–1768. [CrossRef]
77. Jiang, C.; Liu, J.; Zhang, H.; Shi, K. A New Bearing Fault Diagnosis Scheme Using MED-Morphological Filter and Ridge Demodulation Analysis. *J. Vibroeng.* **2015**, *17* , 4231–4247.
78. He, W.; Jiang, Z.; Qin, Q. A Joint Adaptive Wavelet Filter and Morphological Signal Processing Method for Weak Mechanical Impulse Extraction. *J. Mech. Sci. Technol.***2010**, *24*, 1709–1716. [CrossRef]
79. Meng, L.; Xiang, J.; Wang, Y.; Jiang, Y.; Gao, H. A Hybrid Fault Diagnosis Method Using Morphological Filter–Translation Invariant Wavelet and Improved Ensemble Empirical Mode Decomposition. *Mech. Syst. Signal Proc.* **2015**, *50-51*, 101–115. [CrossRef]
80. Yu, J.; Hu, T.; Liu, H. A New Morphological Filter for Fault Feature Extraction of Vibration Signals. *IEEE Access.* **2019**, *7*, 53743–53753. [CrossRef]
81. Hu, Z.; Wang, C.; Zhu, J.; Liu, X.; Kong, F. Bearing Fault Diagnosis Based on an Improved Morphological Filter. *Measurement* **2015**, *80*, 163–178. [CrossRef]
82. Hu, A.; Xiang, L. An Optimal Selection Method for Morphological Filter's Parameters and Its Application in Bearing Fault Diagnosis. *J. Mech. Sci. Technol* **2016**, *30* , 1055–1063. [CrossRef]
83. Wang, J.; Xu, G.; Zhang, Q.; Liang, L. Application of Improved Morphological Filter to the Extraction of Impulsive Attenuation Signals. *Mech. Syst. Signal Proc* **2008**, *23* , 236–245. [CrossRef]
84. Yan, X.; Jia, M. Application of CSA-VMD and Optimal Scale Morphological Slice Bispectrum in Enhancing Outer Race Fault Detection of Rolling Element Bearings. *Mech. Syst. Signal Proc* **2019**, *122*, 56–86. [CrossRef]
85. Van, M.; Franciosa, P.; Ceglarek, D. Rolling Element Bearing Fault Diagnosis Using Integrated Nonlocal Means Denoising with Modified Morphology Filter Operators. *Math. Probl. Eng* **2016**, *1*, 1–14. [CrossRef]
86. Dong, Y.; Liao, M.; Zhang, X.; Wang, F. Faults Diagnosis of Rolling Element Bearings Based on Modified Morphological Method. *Mech. Syst. Signal Proc* **2011**, *25* , 1276–1286. [CrossRef]
87. Raj, A. S.; Murali, N. Early Classification of Bearing Faults Using Morphological Operators and Fuzzy Inference. *IEEE Trans. Ind. Electron* **2013**, *60* , 567–574. [CrossRef]
88. Zhang, X.; Kang, J.; Xiao, L.; Zhao, J. Alpha Stable Distribution Based Morphological Filter for Bearing and Gear Fault Diagnosis in Nuclear Power Plant. *Sci. Technol. Nucl. Install* **2015**, *1*, 1–15. [CrossRef]
89. Osman, S.; Wang, W. A Morphological Hilbert-Huang Transform Technique for Bearing Fault Detection. *IEEE Trans. Instrum. Meas* **2016**, *65* , 2646–2656. [CrossRef]
90. Jingxiang Lv; Yu, J. Average Combination Difference Morphological Filters for Fault Feature Extraction of Bearing. *Mech. Syst. Signal Proc* **2017**, *100*, 827–845. [CrossRef]
91. Li, Y.; Zuo, M. J.; Chen, Y.; Feng, K. An Enhanced Morphology Gradient Product Filter for Bearing Fault Detection. *Mech. Syst. Signal Proc* **2018**, *109*, 166–184. [CrossRef]
92. Li, Y.; Liang, X.; Zuo, M. J. Diagonal Slice Spectrum Assisted Optimal Scale Morphological Filter for Rolling Element Bearing Fault Diagnosis. *Mech. Syst. Signal Proc* **2016**, *85*, 146–161. [CrossRef]
93. Feng, G.-B.; Zhu, Y.-B.; Sun, H.-G. Study on Fault Diagnosis of Gearbox Based on Morphological Filter and Multi-Fractal Theory. *in: Int. Conf. Qual. Reliab. Risk, Maint. Saf. Eng. Xi'an, China* **2011**, 472–477. [CrossRef]
94. Zhou, L. Application of Morphological Demodulation in Gear Fault Feature Extraction. *J. Zhejiang Univ. (Eng. Sci.)* **2010**, *44* , 1514–1518. [CrossRef]

95. Gryllias; C. Yiakopoulos; Antoniadis, I. Application of Morphological Analysis for Gear Fault Detection and Trending. *Diagnostyka* **2008**, 37–42.
96. Qin Shu-ren. HYBRID WAVELET-MORPHOLOGY-EMD ANALYSIS and ITS APPLICATION. *J. Vib. Shock* **2008**.
97. Guo, J.; Zhen, D.; Li, H.; Shi, Z.; Gu, F.; Ball, A. Fault Detection for Planetary Gearbox Based on an Enhanced Average Filter and Modulation Signal Bispectrum Analysis. *ISA Trans* **2020**, *101*, 408–420. [CrossRef]
98. Li, B.; Zhang, P.; Wang, Z.; Mi, S.; Liu, D. A Weighted Multi-Scale Morphological Gradient Filter for Rolling Element Bearing Fault Detection. *ISA Trans* **2011**, *50* , 599–608. [CrossRef]
99. Feng, Y.; Lu, B.; Zhang, D. Multiscale Morphological Manifold for Rolling Bearing Fault Diagnosis. *Proceedings of the Institution of Mechanical Engineers, Mech. Eng. Sci* **2016**, *231* , 3516–3529. [CrossRef]
100. Gong, T.; Yuan, Y.; Yuan, X.; Wu, X. Application of Optimized Multiscale Mathematical Morphology for Bearing Fault Diagnosis. *Meas. Sci. Technol* **2017**, *28* , 045401. [CrossRef]
101. Lv, C.; Zhang, P.; Wu, D.; Li, B.; Zhang, Y. Bearing Fault Signal Analysis Based on an Adaptive Multiscale Combined Morphological Filter. *Int. J. Rotating Mach* **2020**, *1*, 1–8. [CrossRef]
102. Tang, M.; Liao, Y.; He, D.; Duan, R.; Zhang, X. Rolling Bearing Diagnosis Based on an Unbiased-Autocorrelation Morphological Filter Method. *Measurement* **2021**, *189*, 110617–110617. [CrossRef]
103. Gong, T.; Yuan, Y.; Yuan, X.; Wang, X.; Wu, X.; Li, Y. Iterative Asymmetric Multiscale Morphology and Its Application to Fault Detection for Rolling Element Bearing. *Proc. Inst. Mech. Eng. Part C-J. Eng. Mech. Eng. Sci* **2017**, *232* , 316–330. [CrossRef]
104. Li, Y.; Liang, X.; Lin, J.; Chen, Y.; Liu, J. Train Axle Bearing Fault Detection Using a Feature Selection Scheme Based Multi-Scale Morphological Filter. *Mech. Syst. Signal Proc* **2018**, *101*, 435–448. [CrossRef]
105. Yan, X.; Tang, G.; Wang, X. A Chaotic Feature Extraction Based on SMMF and CMMFD for Early Fault Diagnosis of Rolling Bearing. *IEEE Access* **2020**, *8*, 179497–179515. [CrossRef]
106. Qu, X.; Zhang, Y.; Yin, L. Fault Diagnosis for Road Heading Bearings Based on a Multiscale Enhanced Cascaded Difference Filter. *J. Comput. Nonlinear Dyn* **2024**, *19* . [CrossRef]
107. Yu, J.; Xiao, C.; Hu, T.; Gao, Y. Selective Weighted Multi-Scale Morphological Filter for Fault Feature Extraction of Rolling Bearings. *ISA Trans* **2023**, *132*, 544–556. [CrossRef]
108. Li, Y.; Zuo, M. J.; Chen, Z.; Lin, J. Railway Bearing and Cardan Shaft Fault Diagnosis via an Improved Morphological Filter. *Health Monit* **2019**, *19* , 1471–1486. [CrossRef]
109. Zhang, L.; Xu, J.; Yang, J.; Yang, D.; Wang, D. Multiscale Morphology Analysis and Its Application to Fault Diagnosis. *Mech. Syst. Signal Proc* **2008**, *22* , 597–610. [CrossRef]
110. Li, Y.; Xu, M.; Liang, X.; Huang, W.-H. Application of Bandwidth EMD and Adaptive Multiscale Morphology Analysis for Incipient Fault Diagnosis of Rolling Bearings. *IEEE Trans. Ind. Electron* **2017**, *64* , 6506–6517. [CrossRef]
111. Patel, V. N.; Tandon, N.; Pandey, R. K. Improving Defect Detection of Rolling Element Bearings in the Presence of External Vibrations Using Adaptive Noise Cancellation and Multiscale Morphology. *Proc. Inst. Mech. Eng. Part J.-J. Eng. Tribol* **2011**, *226* , 150–162. [CrossRef]
112. Shuai, J.; Shen, C.; Zhu, Z. Adaptive Morphological Feature Extraction and Support Vector Regressive Classification for Bearing Fault Diagnosis. *Int. J. Rotating Mach* **2017**, *1*, 1–10. [CrossRef]
113. Cui, L.; Wang, J.; Ma, J. Early Fault Detection Method for Rolling Bearing Based on Multiscale Morphological Filtering of Information-Entropy Threshold. *J. Mech. Sci. Technol* **2019**, *33* , 1513–1522. [CrossRef]
114. Shen, C.; He, Q.; Kong, F.; Tse, P. W. A Fast and Adaptive Varying-Scale Morphological Analysis Method for Rolling Element Bearing Fault Diagnosis*Proc. Inst. Mech. Eng. Part C-J. Eng. Mech. Eng. Sci.* **2012**, *227* , 1362–1370. [CrossRef]
115. Li, Y.; Liang, X.; Zuo, M. J. A New Strategy of Using a Time-Varying Structure Element for Mathematical Morphological Filtering. *Measurement* **2017**, *106*, 53–65. [CrossRef]
116. Deng, F.; Yang, S.; Tang, G.; Hao, R.; Zhang, M. Self Adaptive Multi-Scale Morphology AVG-Hat Filter and Its Application to Fault Feature Extraction for Wheel Bearing. *Meas. Sci. Technol* **2017**, *28* , 045011–045011. [CrossRef]

 doi:10.20944/preprints202512.0987.v1

117. Yan, X.; Liu, T.; Fu, M.; Ye, M.; Jia, M. Bearing Fault Feature Extraction Method Based on Enhanced Differential Product Weighted Morphological Filtering. *Sensors* **2022**, *22* , 6184. [CrossRef]
118. Wang, S.; Chen, B.; Cheng, Y.; Jiang, X. Investigation on Morphological Filtering via Enhanced Adaptive Time-Varying Structural Element for Bearing Fault Diagnosis. *Measurement* **2025**, *244*, 116466. [CrossRef]
119. Wang, S.; Mei, G.; Chen, B.; Cheng, Y. An Improved Time-Varying Morphological Filtering and Its Application to Bearing Fault Diagnosis. *IEEE Sens. J* **2022**, *22* , 20707–20717. [CrossRef]
120. Li, H.; Zhao, J.; Song, W.; Teng, H. An Offline Fault Diagnosis Method for Planetary Gearbox Based on Empirical Mode Decomposition and Adaptive Multi-Scale Morphological Gradient Filter. *J. Vibroeng* **2015**, *17* , 705–719.
121. Li, B.; Zhang, P. L.; Wang, Z. J.; Mi, S. S.; and Liu, D. S. Gear Fault Detection Using Multi-Scale Morphological Filters. *Measurement.* 2011, *44*, 2078–2089.[CrossRef]
122. Guo, J. C.; Shi, Z. Q.; Li, H. Y.; and He, Z. J. Transient Impulses Enhancement Based on Adaptive Multi-Scale Improved Differential Filter and Its Application in Rotating Machines Fault Diagnosis. *ISA* Trans. 2022, *120*, 271–292. [CrossRef]
123. Wang, J.; Wang, H.; Guo, L.; and Yang, D. Modeling and Fault Identification of the Gear Tooth Surface Wear Failure System. *Int. J. Nonlinear Sci. Numer Simul.* 2021, *22*, 341–351. [CrossRef]
124. Cai, J. H.; and Li, X. Q. Gear Fault Diagnosis Based on Time–Frequency Domain De-Noising Using the Generalized S Transform. *J. Vib. Control.* 2018, *24*, 3338–3347. [CrossRef]
125. Li, Y. B.; Li, G. Y.; Yang, Y. T.; Liang, X. H.; and Xu, M. Q. A Fault Diagnosis Scheme for Planetary Gearboxes Using Adaptive Multi-Scale Morphology Filter and Modified Hierarchical Permutation Entropy. *Mech. Syst. Signal Proc.* 2018, *105*, 319–337. [CrossRef]
126. Wei, Y.; Xu, M.; Wang, X.; Huang, W.; Li, Y. A Hybrid Approach for Weak Fault Feature Extraction of Gearbox. *IEEE Access*. **2019**, *7*, 16616–16625. [CrossRef]
127. Luo, J. S.; Yu, D. J.; and Liang, M. Gear Fault Detection under Time-Varying Rotating Speed via Joint Application of Multiscale Chirplet Path Pursuit and Multiscale Morphology Analysis. *Struct. Health Monit.* 2012, *11*, 526–537. [CrossRef]
128. Zhang, L.; Zhang, L.; Yang, J.; Li, M. Adaptive Morphological Filter to Fault Diagnosis of Gearbox. *in: Int. Conf. Consum. Electron. Communications Netw.* 2011; pp. 70–73. [CrossRef]
129. Yu, J. B.; Huang, J. H.; Liu, C. H.; Li, Z. N.; and Chen, B. Q. Fault Feature of Gearbox Vibration Signals Based on Morphological Filter Dynamic Convolution Autoencoder. *IEEE Sens. J.* 2022, *22,* 22931–22942. [CrossRef]
130. Liu, T. T.; Cui, L. L.; and Zhang, C. Study on Fault Diagnosis Method of Planetary Gearbox Based on Turn Domain Resampling and Variable Multi-Scale Morphological Filtering. *Symmetry* 2021, *13*, 52. [CrossRef]
131. Yan, X.; She, D.; Xu, Y.; and Jia, M. Application of Generalized Composite Multiscale Lempel–Ziv Complexity in Identifying Wind Turbine Gearbox Faults. *Entropy*. 2021, *23*, 1372. [CrossRef]
132. Liu, T. T.; Cui, L. L.; Zhang, J. Y.; and Li, G. Research on Fault Diagnosis of Planetary Gearbox Based on Variable Multi-Scale Morphological Filtering and Improved Symbol Dynamic Entropy. *Int. J. Adv. Manuf. Technol.* 2023,*124*,3947–3961. [CrossRef]
133. Ye, Z.; and Yu, J. B. Deep Morphological Convolutional Network for Feature Learning of Vibration Signals and Its Applications to Gearbox Fault Diagnosis. *Mech. Sys, Signal Proc.* 2021, *161*, 107984.[CrossRef]
134. Cao, S. X.; Li, H. K.; Zhang, K. L.; Zhang, Y.; and Li, Y. F. Strategy for Detection and Suppression of Random Impulse Interferences in Gearbox Vibration Signals. *IEEE Sens.* 2024, *24*, 3523–3539. [CrossRef]
135. Chen, Q.; Chen, Z. W.; Sun, W.; and Li, C. S. A New Structuring Element for Multi-Scale Morphology Analysis and Its Application in Rolling Element Bearing Fault Diagnosis. *J. Vib. Control* 2015, *21*, 765–789. [CrossRef]
136. Gao, J. W.; Wang, R. C.; Zhang, R. L.; Li, H. F.; and Li, H. B. A Novel Fault Diagnosis Method for Rotating Machinery Based on S Transform and Morphological Pattern Spectrum. *J. Braz. Soc. Mech. Sci. Eng.* 2016, *38*, 1575–1584. [CrossRef]
137. Sun, D.; Wang, B.; Hu, X.; and He, Q. B. A Fault Diagnosis Method Based on Improved Pattern Spectrum and FOASVM. *In. J. Acous. Vib.* 2019, *24*, 312–319. [CrossRef]

 doi:10.20944/preprints202512.0987.v1

138. Zhu, W. Y.; Zhang, W. X.; and Zhang, C. Rolling Bearing Fault Diagnosis Based on Mathematical Morphological Spectrum. In *Mechanism and Machine Science*; **2023**; *129*, pp 688–698. [CrossRef]
139. Li, Y. F.; Zuo, M. J.; and Li, Y. B. Application of Modified Morphological Pattern Spectrum and LSSVM for Fault Diagnosis of Train Wheelset Bearings. In *International Conference on Sensing, Diagnostics, Prognostics, and Control*; Xi'an, China, **2018**; pp 50–55.[CrossRef]
140. Gao, J.; Tao, L.; Zhang, M.; and Wang, R. C. New Time-Frequency Representations Based on the Morphological Pattern Spectrum for Bearing Fault Diagnosis. In *7th International Conference on Computational Methods*; California, USA, **2016;** pp 213–231.
141. Hao, R. J.; Peng, Z. K.; Feng, Z. P.; Zhang, X. H.; and Chu, F. L. Application of Support Vector Machine Based on Pattern Spectrum Entropy in Fault Diagnostics of Rolling Element Bearings. *Meas. Sci. Technol.* 2011, *22*, 045708. [CrossRef]
142. Hao, R. J.; Feng, Z. P.; and Chu, F. L. Defects Diagnosis and Classification for Rolling Bearing Based on Mathematical Morphology. In *8th International Conference on Reliability, Maintainability and Safety*; Chengdu, China, **2009**; pp 817–821. [CrossRef]
143. Wang, W. J.; Cui, L. L.; and Chen, D. Y. Multi-Scale Morphology Analysis of Acoustic Emission Signal and Quantitative Diagnosis for Bearing Fault. *Acta Mech. Sin.* 2016, *32*, 265–272. [CrossRef]
144. Yu, X. T.; Lu, W. X.; and Chu, F. L. Fault Diagnostics Based on Pattern Spectrum Entropy and Proximal Support Vector Machine. *Key Eng. Mater.* 2009, *413*, 607–612. [CrossRef]
145. Yan, X.; Liu, Y.; Ding, P.; Jia, M. P.; and Li, Y. B. Fault Diagnosis of Rolling-Element Bearing Using Multiscale Pattern Gradient Spectrum Entropy Coupled with Laplacian Score.*Complexity,* 2020, *1*, 1–29. [CrossRef]
146. Zhao, H. M.; Yao, R.; Xu, L.; Yuan, Y. B.; and Li, Y. B. Study on a Novel Fault Damage Degree Identification Method Using High-Order Differential Mathematical Morphology Gradient Spectrum Entropy. *Entropy* 2018, *20*, 682. [CrossRef]
147. Zhao, H. M.; Liu, H. D.; Xu, J. J.; and Li, Y. B. Performance Prediction Using High-Order Differential Mathematical Morphology Gradient Spectrum Entropy and Extreme Learning Machine. *IEEE Tran. Instrum. Meas.* 2020, *69*, 4165–4172. [CrossRef]
148. Li, H. R.; Wang, Y. K.; Wang, B.; Luo, M. Y.; and Li, Y. B. The Application of a General Mathematical Morphological Particle as a Novel Indicator for the Performance Degradation Assessment of a Bearing. *Mech. Syst. Signal Proc.* 2017, *82*, 490–502. [CrossRef]
149. Gao, H.; Liu, J.; Li, Y. A New Approach for Performance Degradation Feature Extraction Based on Generalized Pattern Spectrum Entropy. *Proc. Inst. Mech. Eng. Part C-J. Mech. Eng. Sci.* **2015**, *231*, 1932–1945. [CrossRef]
150. Wang, B.; Wang, W.; Hou, M. H.; Li, H. R.; and Li, Y. B. Bearing Performance Degradation Condition Recognition Based on a Combination of Improved Pattern Spectrum Entropy and Fuzzy C-Means. *J. Intell. Fuzzy Syst.* 2018, *34*, 3681–3693. [CrossRef]
151. Li, B.; Gao, M.; Guo, Q.; Zhang, P. L.; and Liu, D. S. Characterizing Vibration Signals Utilizing Morphological Pattern Spectrum for Gear Fault Diagnosis. In *3rd International Conference on Mechatronics, Robotics and Automation*; Shenyang, China, **2015**; pp 707–711. [CrossRef]
152. Li, B.; Zhang, P-L.; Wang, Z-J.; Mi, S-S.; Liu, D-S. Application of S Transform and Morphological Pattern Spectrum for Gear Fault Diagnosis. *Proc. Inst. Mech. Eng. Part C-J. Eng. Mech. Eng. Sci.* **2011**, *225*, 2963–2972. [CrossRef]
153. Barbieri, N.; Barbieri, G.; Martins, B.; Sant'Ana, R.; and De Lacerda De Oliveira, L. Analysis of Automotive Gearbox Faults Using Vibration Signal. *Mech. Syst. Signal Process.* 2019, *129*, 148–163. [CrossRef]
154. Hao, R. J.; and Chu, F. L. Morphological Undecimated Wavelet Decomposition for Fault Diagnostics of Rolling Element Bearings. *J. Sound Vibr.* 2009, *320*, 1164–1177. [CrossRef]
155. Wang, S.; and Zhou, J. Fault Diagnosis of Rolling Bearing Based on Lifting Morphological Wavelet and Ensemble Empirical Mode Decomposition. In *International Conference on Consumer Electronics, Communications and Networks*; Xining, China, **2011**; pp 2229–2232. [CrossRef]
156. Li, B.; Zhang, P. L.; Mi, S. S.; Liu, D. S.; and Ren, Y. Q. An Adaptive Morphological Gradient Lifting Wavelet for Detecting Bearing Defects. *Mech. Syst. Signal Proc.* 2012, *29*, 415–427. [CrossRef]

 doi:10.20944/preprints202512.0987.v1

157. Li, C.; Liang, M.; Zhang, Y.; and Hou, S. Multi-Scale Autocorrelation via Morphological Wavelet Slices for Rolling Element Bearing Fault Diagnosis. *Mech. Syst. Signal Proc.* 2012, *31*, 428–446. [CrossRef]
158. Chen, Q. H.; Li, H. R.; and Xu, B. H. An Improved Multi-Scale Morphological Undecimated Wavelet Method and Its Application in Rolling Bearing Fault Feature Extraction. *Appl. Mech. Mater*. 2013, *380*, 1009–1013. [CrossRef]
159. Han, X.; Xiong, J.; Sun, R.; and Chen, Y. C. Research on the Roller Bearing Fault Diagnosis Based on Morphological Wavelet and LSSVM Algorithm. In *International Conference on Quality, Reliability, Risk, Maintenance, and Safety Engineering*; Mingshan, China, **2013**; pp 1888–1892.
160. Meng, L. J.; Xiang, J. W.; Zhong, Y. T.; and Wang, Y. Y. Fault Diagnosis of Rolling Bearing Based on Second Generation Wavelet Denoising and Morphological Filter. *J. Mech. Sci. Technol.* 2015, *29*, 3121–3129. [CrossRef]
161. M.H. Khakipour; Safavi, A. A.; P. Setoodeh. Bearing Fault Diagnosis with Morphological Gradient Wavelet. *J. Frankl. Inst.* **2016**, *354*, 2465–2476. [CrossRef]
162. Li, Y.; Liang, X.; Liu, W.; Wang, Y. Development of a Morphological Convolution Operator for Bearing Fault Detection. *J. Sound Vib.* **2018**, *421*, 220–233. [CrossRef]
163. Guo, J.; He, Q.; Zhen, D.; Gu, F.; Ball, A. D. An Iterative Morphological Difference Product Wavelet for Weak Fault Feature Extraction in Rolling Bearing Fault Diagnosis. *Struct. Health Monit.* **2022**, 2222, 296-318. [CrossRef]
164. Li, Y.; Feng, K.; Chen, Y.; Chen, Z. Multioperator Morphological Undecimated Wavelet for Wheelset Bearing Compound Fault Detection. *IEEE Trans. Instrum. Meas.* **2023**, *72*, 1–12. [CrossRef]
165. Li, H.; Tan, Y.; Pu, Y. Rolling Bearing Fault Vibration Signal Denoising Based on Adaptive Morphological Wavelet Perona–Malik Filter Algorithm. *Shock Vib.* **2021**, *2021*. [CrossRef]
166. Duan, R.; Liao, Y.; Yang, L.; Song, E. Faulty Bearing Signal Analysis with Empirical Morphological Undecimated Wavelet. *IEEE Trans. Instrum. Meas.* **2022**, *71*, 1–11. [CrossRef]
167. Wang, H.; Ji, X.; Wang, X.; Li, Z.-N. Fault Feature Extraction of Fan Bearing Based on Improved Mathematical Morphological Unsampled Wavelet. *Chin. Autom. Congress*. **2017**, *33*, 3188–3192. [CrossRef]
168. Zhang, W.; Shen, L.; Li, J.; Cai, Q.; Wang, H. Morphological Undecimated Wavelet Decomposition for Fault Feature Extraction of Rolling Element Bearing. In *2009 2nd International Congress on Image and Signal Processing*; IEEE, 2009; pp. 1–5. [CrossRef]
169. Yong, L. Rolling Bearing Fault Diagnosis Based on Morphological Wavelet Theory and Bi-Spectrum Analysis. *J. Zhejiang Univ-Eng. Sci.* **2010**, *44*, 432–439. [CrossRef]
170. Yang, X.; Zhou, X.; Zhang, W.; Yang, F.; Lin, Y. Rolling Bearing Fault Feature Extraction Based on Morphological Wavelet and S-Transform. *J. Zhejiang Univ-Eng. Sci.* **2010**, *44*, 2088–2092. [CrossRef]
171. Li, B.; Zhang, P.; Mao, Q.; Mi, S.; Liu, P. Gear Fault Detection Using Adaptive Morphological Gradient Lifting Wavelet. *J. Vib. Control.* **2012**, *19*, 1646–1657. [CrossRef]
172. Zhang, W. B.; Su, Y. P.; Zhou, Y. J.; Pu, Y. S. A New Intelligent Fault Recognition Method for Gearbox. *Adv. Mater. Res.* **2013**, *684*, 369–372. [CrossRef]
173. Hong, S.; Fang-jian, S.; Bo, C.; Wei, Q. Research of Gear Fault Detection in Morphological Wavelet Domain. *J. Phys. Conf. Ser.* **2016**, *679*, 012035. [CrossRef]
174. Zhang, W.; Pu, Y.; Guo, D.; Jiang, J.; Yu, L.; Min, J. Application of Morphological Wavelet and Permutation Entropy in Gear Fault Recognition. *Evol. Intell.* **2020**, *15*, 2427–2436. [CrossRef]
175. Cai, J.; Wang, X. Crack Fault Diagnosis of Gear Based on Morphological Wavelet De-Noising. J. Mech. Strength. **2015**, *37*, 398–402.
176. Ding, W.; Zhang, Z.; Yao, L.; Huang, J. Fault Recognition Method of Transmission Gear Based on Morphological Wavelet and Permutation Entropy. *J. Mech. Transm.* **2019**, *43*, 165–168.
177. Zhang, P.; Li, B.; Zhang, Y.; Mi, S.; Liu, D. Max-Lifting Morphological Wavelet Transform Based Gear Fault Feature Extraction. *Chin. J. Sci. Instrum.* **2010**, *31*, 2736-2741.
178. Tong, R.; Kang, J.; Li, B.; Sun, J. A Preprocessing Method for the Vibration Signal of Gear Based on MUDW and CK. In *2017 9th International Conference on Modelling, Identification and Control (ICMIC)*; 2017; pp. 680–686. [CrossRef]

 doi:10.20944/preprints202512.0987.v1

179. Shen, L.; Zhou, X.; Liu, L.; Yang, F. Application of Morphological Wavelet De-noising in Extracting Gear Fault Feature, *Trans. Chin. Soc. Agr. Mach.* **2010**, *41*, 217-221. [CrossRef]
180. Li, Y.-F.; Zuo, M.; Feng, K.; Chen, Y.-J. Detection of Bearing Faults Using a Novel Adaptive Morphological Update Lifting Wavelet. *Chin. J. Mech. Eng.* **2017**, *30*, 1305–1313. [CrossRef]
181. Li, Y.; Zuo, M. J.; Lin, J.; Liu, J. Fault Detection Method for Railway Wheel Flat Using an Adaptive Multiscale Morphological Filter. *Mech. Syst. Signal Proc.* **2017**, *84*, 642–658. [CrossRef]
182. Jiang, W.; Zheng, Z.; Zhu, Y.; Li, Y. Demodulation for Hydraulic Pump Fault Signals Based on Local Mean Decomposition and Improved Adaptive Multiscale Morphology Analysis. *Mech. Syst. Signal Proc.* **2015**, *58-59*, 179–205. [CrossRef]
183. Li, B.; Mi, S.; Liu, P.; Wang, Z. Classification of Time-Frequency Representations Using Improved Morphological Pattern Spectrum for Engine Fault Diagnosis. *J. Sound Vib.* **2013**, *332*, 3329–3337. [CrossRef]
184. Chen, B.; Cheng, Y.; Zhang, W.; Mei, G. Investigation on Enhanced Mathematical Morphological Operators for Bearing Fault Feature Extraction. *ISA Trans. ISA Trans.* **2021**, *126*, 440-459. [CrossRef]